Contemporary Mathematics
https://ojs.wiserpub.com/index.php/CM/

Research Article

A Front Fixing Crank-Nicolson Finite-Difference for the Solvability of the American Put Option Models

Zakaria Idriss Ali*, Minyahil Abera Abebe

Department of Mathematical Sciences, College of Science, Engineering and Technology, School of Science, University of South Africa, Johannesburg, 0003, South Africa
E-mail: alizi@unisa.ac.za

Received: 25 February 2025; **Revised:** 13 March 2025; **Accepted:** 30 April 2025

Abstract: In this paper, a new approach to solve the American put option pricing model has been discussed. The method is based on the front-fixing Crank-Nicolson finite-difference method with the reliance on the Caputo-Fabrizio stochastic fractional derivative with regular kernel. The American put option pricing model is one of the most important models used in finance to determine the value of an option that gives the holder the right to sell an underlying asset at a given price. The approach in this paper deals with early exercise through the use of front-fixing technique that makes it easier and more effective to compute values of American put options. To this end, the method presented here is shown to be stable, precisely effective, and efficient as compared to the existing methods in the literature. Numerical experiments performed also confirm the efficiency of the suggested method and its capability to provide reliable and accurate prices of American put options using a stable scheme.

***Keywords*:** stochastic fractional partial differential equations, American put option, finite-difference, step-size discretization, front-fixing method, consistency and stability

MSC: 65H15, 26A33, 65M06

1. Introduction

The American put option model is one of the most common derivatives instruments that are used in the valuation of financial contracts. This type of option allows investors to exercise their options values at any time before the option expires. This gives the American put option activity an edge over any other options in the market. Hence, European put options are important terms to understand the value and the valuation of American put options in the derivatives market. As for further reading on this particular subject, one can turn to Riccardo et al. [1] and Company et al. [2], for instance.

The foundational work on pricing options via Partial Differential Equations (PDEs), with some stringent assumptions, was principally developed by Black and Scholes and by Merton in the celebrated work [3, 4], respectively, where further details concerning the put options and more references can be found.

Among others, the work of Schwartz in [5], and Brennan and Schwartz in [6, 7], were pioneers in solving American Put Option (APO) problems using the finite-difference method, the accuracy of which has been verified by Jaillet et al. [8]. Further, we acknowledge that subsequent developments done by Company et al. [2], Riccardo et al. [1], Han

DOI: https://doi.org/10.37256/cm.7120268649

and Wu [9], Pantazopoulos et al. [10], and Tangman et al. [11] has considered front tracking methods for monitoring the boundaries and for discretizing the problem within a changing domain for new fractional differential equations with various applications in different fields of science, we refer to recent developments [3, 12–14].

However, we must emphasize that the complexity in pricing American put options stems from determining the optimal time to exercise the underlying asset and from solving a PDE that satisfies the requisite initial and boundary conditions; meaning that, we must closely monitor both the fixed and the unknown free boundary conditions in order to clearly understand the dynamics of the underlying problem. The front-fixing method, which is predicated on a variable change that maps the changing domain to a fixed one, can mitigate the challenges associated with free boundary problems.

A plethora of free boundary problems encountered in physics and finance have been resolved using the Front Fixing Method (FFM), see for instance [1, 2, 11, 15–19] and the references therein. Additionally, similar results with seminal applications and solutions to free boundary option pricing using FFM was observed by Wu and Kwok in their investigation in [18]. The FFM is advantageous for directly computing free boundary problems by simplifying the management of computational mesh points or elements when applying finite-difference and finite-element methods to such problems. This has motivated Landau in his work [20] to highlight that the method effectively transforms unknown, time-varying boundaries into known and fixed boundaries by altering the original problem into a nonlinear PDE within a bounded domain.

The application of fractional calculus has been instrumental in streamlining the modeling of complex systems across various disciplines, with its role intensifying over the past decade in sectors such as finance and economics, among other fields of science, and engineering; where further details can be found in [21–27]. The work by Nuugulu et al. in [28] present a robust numerical approach for solving the fractional Black-Scholes equation applied to pricing American put options. Their method integrates fractional calculus with an implicit front-fixing algorithm, effectively addressing the complexities of the free boundary problem. The results of their study demonstrate that the proposed scheme is consistent, stable, and convergent. However, we need to clearly emphasize that the first work dealing with robust numerical approaches for solving the fractional Black-Scholes differential equations with applications to pricing American put options was dully observed in the paper [29] which to the best of our knowledge was the first paper dealing with robust numerical schemes in establishing not only the existence and uniqueness of solutions to APO but also the deep investigations of their numerical treatment. The current study in this manuscript generalizes to some extends the results in the existing literature as well as some of the work in our ground breaking paper [29].

Having said that, we can also note that valuation of APO contracts have garnered significant attention from financial engineers and mathematicians and other scientists over the past few decades due to their status as one of the most actively traded instruments in the financial options market.

In this article, we apply the new Caputo fractional derivatives, which do not possess a singular kernel (no blow-up at any time), as compared to the classical Black-Scholes equations. Additionally, we introduce a Crank-Nicolson finite-difference scheme combined with the Front-Fixing Method (FFM) to address the challenges in solving the American put options. This study focuses on developing a novel American put option scheme that employs the Crank-Nicolson finite-difference approach and the FFM, specifically in the absence of dividend payments. The proposed method transforms the variable domain problem into a fixed rectangular domain for the nonlinear problem using a front-fixing transformation.

This study underscores the importance of accurate and efficient numerical methods for option pricing. Among the various methods, we introduce a new variant of the Crank-Nicolson finite-difference method, dubbed the front-fixing Crank-Nicolson finite-difference method. This method is designed to navigate the complexities of the early exercise feature of American put options, where the optimal exercise boundary is unknown a priori. We refer the reader to [11, 17] for further elaboration on this method. By integrating front-fixing techniques into the Crank-Nicolson scheme, we propose an enhanced numerical approach that captures the behavior of the early exercise boundary more effectively.

Furthermore, this research augments the ongoing efforts and the extant literature by developing robust and efficient numerical schemes for pricing American put options. This contribution will provide valuable insights for financial practitioners, researchers, and investors engaged in option valuation and portfolio management.

The manuscript is organized as follows: section 2 elaborates on the Caputo-time fractional equation of APO. In section 3, we introduce the fixed domain transformation of the American Put option problem and the Crank-Nicolson discretization of the transformed equation. In section 4 we examine the stability and consistency of the scheme concerning time at the optimal exercise boundary. Section 5 presents numerical experiments and comparisons with other methodologies. Section 6 deals with the managerial and policy implications. Finally, section 7 focuses on concluding and discussing the main results.

2. Time-Caputo-fractional equation of APO

2.1 *The American put options model*

Let us assume that an underlying asset has a price of X at time t. Here, we consider the following mathematical model for the value of an APO to sell the asset $V(X, \tau)$. Therefore, for this purpose, we consider the following problem

$$\begin{cases} \dfrac{\partial V}{\partial \tau} + \dfrac{1}{2}\sigma^2 X^2 \dfrac{\partial^2 V}{\partial^2 X} + rX\dfrac{\partial V}{\partial X} = rV, \text{ for } X = X^*(\tau), \text{ and } t \in [0, T], \\ V(X, T) = \max\{E - X, 0\}, \text{ for } X \geq 0, \\ \dfrac{\partial V}{\partial X}(X^*(\tau), \tau) = -1, \\ V(X^*(\tau), \tau) = E - X^*(\tau), \\ \lim\limits_{X\to\infty} V(X, T) = 0, \\ X^*(T) = E, \\ V(X(\tau), \tau) = E - X, \text{ for } X \in [0, X^*(\tau)), \end{cases} \tag{1}$$

where T is the time horizon which represents the maturity T also known to us sometimes as the expiration time, $t \geq 0$ stands for the time from 0 up to maturity T, $\tau = T - t$ represents the period until maturity T, here, $X^*(t)$ denotes the unknown early exercise-free boundary which we assume that is positive "a priori", i.e., $X^*(t) > 0$, E is the strike price, σ is the volatility parameter and r is the interest rate or simply called the risk-free.

Note that to describe the problem at hand we refer to the Black-Scholes-Merton equation (1) which was initially developed by Black and Scholes [3] and Merton [4], respectively.

2.2 *Derivation of the time Caputo fractional of APO*

This section deals with the fundamental basic definitions of fractional derivatives, focusing especially on the Riemann-Liouville, Caputo, Caputo-Fabrizio and Jumarie derivatives which are not necessarily all investigated in this paper. Our work can literally be extended to these operators and our method can be easily adapted to yield novel results. Subsequently, in this work we must emphasize that the derivation of the time-fractional Black-Scholes Partial Differential Equation (PDE) for pricing American put options without considering dividends is discussed. Finally, the classical American put option pricing model, described by equation (1), has been converted in order to incorporate Caputo-Fabrizio fractional derivatives with much regular kernel as compared to the existing fractional derivatives such as the conformable derivatives as discussed in the respective references [30, 31], the Abu-Shady-Kaabar fractional derivatives in [32] just to mention a few.

2.2.1 *Mathematical preliminaries on fractional differential operators*

The mathematical foundation of fractional calculus has evolved significantly in the recent decades, driven by diverse formulations of fractional-order derivatives designed to address theoretical and applied challenges across several disciplines. This review highlights key formulations rather than providing an exhaustive catalog, focusing on their strengths, limitations, and interdisciplinary relevance.

Among the earliest and most widely used formulations is the Riemann-Liouville derivative, defined via an integral operator with a singular kernel. This approach is well suited for theoretical analysis in mathematical sciences, particularly for solving fractional differential equations and modeling memory-dependent systems, we refer for instance to the work in [33] where the formulation and the theoretical methods of the general fractional derivatives with their applications is widely discussed. However, its incompatibility with standard initial conditions restricts its applicability in physical and engineering models, where classical boundary value frameworks are often required. Despite this limitation, it remains fundamental in solving fractional differential equations and modeling memory-dependent systems (see [33] for further details).

The Caputo derivative addresses the limitations of the Riemann-Liouville formulation by incorporating initial conditions in a form such as classical calculus. This modification enables intuitive interpretations of real-world phenomena, making it more applicable in several areas of physics, finance, and engineering, just to name a few. We must emphasis that its ability to model non-local memory effects (i.e., system behavior dependent on past states) while preserving mathematical tractability has led to widespread adoption in dynamic systems and boundary value problems as observed in [34]. However, its reliance on smoothness assumptions for the integrand can limit its utility in modeling discontinuous or highly irregular processes. This gives new directions for further investigations of the theory in this direction. Nonetheless, this has led to the well-known Abu-shady-Kaabar theory which is explained in great details in [32]. To be more precise, the Abu-Shady-Kaabar fractional derivative builds upon the practicality of the Caputo derivative by incorporating weighted kernels, enhancing flexibility in modeling multi-scale phenomena. Adjusting the kernel function improves adaptability to systems with evolving memory effects, such as signal processing and biological modeling as suggested in the paper [32]. However, its reliance on kernel customization increases computational demands and may limit extension of prospective directives as compared to the classical formulations. Despite these trade-offs, it bridges the classical and modern fractional operators, offering improved accuracy in applications such as visco-elastic material and the characterization of signal processing and biological modeling, see e.g., [32] where further discussion and references can be found therein.

A pivotal advancement in fractional calculus is the Atangana-Baleanu (AB) fractional derivative, which replaces singular kernels with Mittag-Leffler functions to eliminate singularities at the origin. Besides this, the notion of new fractional derivatives with non-local and non-singular kernel was duly studied in [24] where application to heat transfer was investigated. This non-singular operator has transformed the modeling of systems with fading memory, such as visco-elastic materials and financial markets exhibiting long-range dependence. Furthermore, comparative studies in [35] have highlighted the trade-offs between singular and non-singular operators, with the latter offering improved numerical stability at the cost of increased algebraic complexity. Noting that specialized numerical techniques are often required to manage its computational overhead costs, particularly in large-scale simulations, see [24] for further details and subsequent development in this direction.

For a comprehensive discussion of fractional derivatives, their theoretical foundations, and their respective advantages and limitations, we refer to [35] where the advantages and disadvantages of the classical fractional order derivations were clearly observed and moreover, the authors have also proposed a new alternative fractional order derivative which have been applied to some special functions to validate its theory and applications in [26]. Further analyzes of fractional calculus, along with methodological developments and applications, can be obtained in [36] where further results using the modified Riemann-Liouville derivative and fractional Taylor series applied to some non-differentiable function have also been discussed. Among others, we mention the work in [37] which deals with the stock exchange fractional order dynamics and the stock was modeled using the non-random fractional processes subjected to real-valued Brownian motion that can be used to model fractional Black-Scholes differential equations, and [38] where a new families of fractional Black-Scholes equations are modeled based on the fractional processes governed by Gaussian white noise. Additional insightful discussions on specific fractional derivatives and robust numerical schemes can be found in [29, 33, 34, 36, 37, 39]. Although this review is not exhaustive, it highlights key developments in fractional calculus. For a more complete list of fractional derivatives, we refer to [29], which provides recent citations and additional references. To this end we present the following concept:

Definition 1 New Caputo Fractional Derivative

Let $v : \mathbb{R} \to \mathbb{R}$ be a continuous but not necessarily differentiable function. The Caputo fractional derivative of order α is defined as follows (for more details concerning this definition we refer for instance to the papers [24, 26, 40–42]):

$$\frac{\partial^\alpha v}{\partial t^\alpha} = {}_0^cD_t^\alpha v(\tau, y) = \frac{1}{(1-\alpha)} \int_0^t v'(\tau) e^{-\frac{\alpha(t-\tau)}{1-\alpha}} d\tau. \tag{2}$$

We remark from the above definition that the presence of the function v' which is the derivative of the function v. Note that this already suggest to us that the classical derivative of the function v must exist before we can apply this definition. Most recent remarks on the definitions of fractional derivatives are clearly highlighted in the recent manuscript [40].

Definition 2 Caputo Fractional Derivative

Let $v : \mathbb{R} \to \mathbb{R}$ be a continuous but not necessarily differentiable function. The Caputo fractional derivative of order α is defined as follows:

$$\frac{\partial^\alpha v}{\partial t^\alpha} = {}_0^cD_t^\alpha v(\tau, y) = \frac{1}{\Gamma(1-\alpha)} \int_0^t v'(\tau) \frac{1}{(t-\tau)^{\alpha-1}} d\tau$$

$$D_t^\alpha v(t) = \frac{1}{\Gamma(\eta-\alpha)} \int_0^t \frac{d^\eta v(\tau)}{d\tau^\eta} (t-\tau)^{\alpha-\eta+1} d\tau, \quad \eta - 1 < \alpha \leq \eta; \quad \eta \in \mathbb{N}. \tag{3}$$

We remark that a key advantage of the Caputo fractional derivative is its ability to incorporate classical initial and boundary conditions into the problem formulation.

Definition 3 Riemann-Liouville Fractional Derivative

Let $v : \mathbb{R} \to \mathbb{R}$ be a continuous but not necessarily differentiable function. Then, the Riemann-Liouville fractional derivative of order α is given by:

$$D_t^\alpha v(t) = \frac{1}{\Gamma(\eta-\alpha)} \frac{d^\eta}{dt^\eta} \int_0^t v(\tau)(t-\tau)^{\alpha-\eta+1} d\tau, \quad \eta - 1 < \alpha \leq \eta; \quad \eta \in \mathbb{N}. \tag{4}$$

We notice that the Riemann-Liouville derivative exhibits certain limitations when modeling real-world phenomena. Specifically, it produces a non-zero derivative for a constant and introduces singularities at the origin when the function remains constant at that point, as observed with exponential and Mittag-Leffler functions. These challenges constraint its applicability. However, it was demonstrated in [36] that modifications to the Riemann-Liouville definition can address some of these issues.

Definition 4 Jumarie (Modified Riemann-Liouville) Derivative

Let $v : \mathbb{R} \to \mathbb{R}$ be a continuous, but not necessarily differentiable function. The Jumarie fractional derivative of order α is defined as follows:

i. If $v(t) := K$ is a constant function, then its Jumarie fractional derivative is given by:

$$D_t^{\alpha} v(t) = \begin{cases} \dfrac{K}{\Gamma(\eta-\alpha)} t^{-\alpha+1-\eta}, & \alpha \leq \eta - 1, \\ \\ 0, & \alpha > \eta - 1, \end{cases} \tag{5}$$

where $\eta \in \mathbb{N}$ and Γ is the Gamma function.

ii. If $v(t)$ is not a constant function, then its fractional derivative is defined by:

$$D_t^{\alpha} v(t) = \frac{1}{\Gamma(\eta-\alpha)} \frac{d^{\eta}}{dt^{\eta}} \int_0^t \frac{v(\tau)-v(0)}{(t-\tau)^{\alpha}} d\tau, \quad \eta - 1 < \alpha \leq \eta, \tag{6}$$

where $\eta \in \mathbb{N}$.

Definition 5 Fractional Taylor Series

Let $v : \mathbb{R} \to \mathbb{R}$ be a continuous function that has a derivative of order $\alpha\zeta$, where ζ is any positive integer, and $0 < \alpha \leq 1$. The fractional Taylor series is given by:

$$v(t+\kappa) = \begin{cases} \sum_{\zeta=0}^{\infty} \dfrac{\kappa^{\alpha\zeta}}{\Gamma(1+\alpha\zeta)} v^{(\alpha\zeta)}(t), & \eta - 1 < \alpha \leq \eta, \\ \\ v(t) + \kappa v'(t) + \sum_{\zeta=1}^{\infty} \dfrac{\kappa^{\zeta}\beta_e + 1}{\Gamma(\zeta\beta_e + 2)} v^{(\zeta\beta_e+1)}(t), & \beta_e = \alpha - \eta, \end{cases} \tag{7}$$

where $\eta \in \mathbb{N}$.

2.3 *Derivation of the time-fractional Black-Scholes PDE*

Before delving into the derivation of the time-fractional stochastic partial differential equations, we need to introduce one important ingredient in stochastic calculus, the Itô's lemma. To frame our approach, we first define the Itô's lemma. The later is widely used in the subsequent analysis. For a comprehensive discussion, we refer to the celebrated book [43] where the stochastic partial differential equations were introduced and further discussed in great details.

Lemma 1 Itô's Lemma

Let X_t be an Itô process given by

$$dX = \mu(X, t)\, dt + \sigma(X, t)\, dW_t \tag{8}$$

where W_t is a standard Wiener process, and $\mu(X, t)$ and $\sigma(X, t)$ are sufficiently smooth functions. Let $f(t, x) \in C^2([0, \infty) \times \mathbb{R})$, i.e., f is twice continuously differentiable on $[0, \infty) \times \mathbb{R}$. Then the process $f(X, t)$ is again an Itô's process, and its differential is given by

$$df = \left(\frac{\partial f}{\partial t} + \mu \frac{\partial f}{\partial X} + \frac{1}{2}\sigma^2 \frac{\partial^2 f}{\partial X^2} \right) dt + \sigma \frac{\partial f}{\partial X} dW_t. \tag{9}$$

For the proof of this lemma, we refer to [43].

In the derivation of the time-fractional Black-Scholes Partial Differential Equation (tfBS-PDE), we start by assuming that the stock price dynamics follow the fractional stochastic equation:

$$dX = rX\, dt + \sigma\omega(t)(dt)^{\alpha/2}, \quad 0 < \alpha \leq 1, \tag{10}$$

where X is the stock price, σ is the volatility, r is the risk-free interest rate, and $\omega(t)$ represents a standard Wiener process. Arguing similarly as in [22, 28], we can assert that using Jumarie's fractional Taylor series, as defined in (7), the following identities can be derived:

$$d^{\alpha}t = \frac{1}{\Gamma(2-\alpha)} t^{1-\alpha}(dt)^{\alpha}, \quad 0 < \alpha \leq 1, \tag{11}$$

$$d^{\alpha}X = \Gamma(1+\alpha)dX, \quad 0 < \alpha \leq 1, \tag{12}$$

$$\frac{d^{\alpha}X}{(dX)^{\alpha}} = \frac{1}{\Gamma(2-\alpha)} X^{1-\alpha}, \quad 0 < \alpha \leq 1. \tag{13}$$

Combining equations (11) and (13) results in a formula that enables the conversion between integer-order and fractional-order derivatives.

$$dX = X^{1-\alpha}\frac{\Gamma(1+\alpha)}{\Gamma(2-\alpha)}(dX)^{\alpha}, \quad 0 < \alpha \leq 1. \tag{14}$$

Now, let $V(X, t)$ be the value of an American put option, and assume that $V(X, t)$ satisfies the following assumption:

Assumption 1 The function $V(X, t)$ is sufficiently smooth with respect to X, and its fractional derivative with respect to time exists for some $\alpha \in (0, 1)$.

Remark 1 We notice that in the aforementioned definitions, we used the condition $0 < \alpha \leq 1$. However, in the condition given in the above assumption, the case $\alpha = 1$ was not considered due to the fact that when $\alpha = 1$ the result applies to the classical derivative and there will no confusion to make.

The dynamics of the risk-free investment interest rate are given by:

$$dV = rV\, dt.$$

Multiplying both sides of this equation by $\Gamma(1+\alpha)$, we obtain:

$$\Gamma(1+\alpha)dV = \Gamma(1+\alpha)rV\, dt. \tag{15}$$

Using equation (15) and combining it with (11), we derive the following fractional interest rate increment:

$$d^{\alpha}V = \Gamma(1+\alpha)rV\, dt. \tag{16}$$

Now, combining equations (16) and (14), we obtain the fractional interest rate dynamic equation:

$$d^{\alpha}V = rV\frac{1}{\Gamma(2-\alpha)}t^{1-\alpha}(dt)^{\alpha}. \tag{17}$$

Since $V(X, t)$ is sufficiently smooth, applying the fractional Taylor series expansion (7) of order α on $V(X, t)$, we obtain

$$dV = \frac{1}{\Gamma(1+\alpha)}\frac{\partial^{\alpha}V}{\partial t^{\alpha}}(dt)^{\alpha} + \frac{\partial V}{\partial X}dX + \frac{1}{2}\frac{\partial^2 V}{\partial X^2}(dX)^2. \tag{18}$$

Now we can apply Itô's lemma on (10) to find $(dX)^2$

$$(dX)^2 = \left(rX\,dt + \sigma\omega(t)\,(dt)^{\alpha/2}\right)^2$$

$$(dX)^2 = (rX\,dt)^2 + 2\,(rX\,dt)\left(\sigma\omega(t)\,(dt)^{\alpha/2}\right) + \left(\sigma\omega(t)\,(dt)^{\alpha/2}\right)^2$$

$$(dX)^2 = 2rX\sigma\omega(t)(dt)^{1+\alpha/2} + \sigma^2\omega(t)^2\,(dt)^{\alpha} \quad \text{since} \quad (dt)^2 = 0 \tag{19}$$

In Itô's calculus, $(dt)^{1+\alpha/2}$ is a higher-order term and vanishes. Since $\omega(t)$ is a stochastic process with $\omega(t)^2 \sim 1$, the term $\left(\sigma\omega(t)\,(dt)^{\alpha/2}\right)^2$ simplifies to $\sigma^2(dt)^{\alpha}$.

Hence, (19) becomes

$$(dX)^2 = \sigma^2(dt)^{\alpha} \tag{20}$$

Plugging equation (20) and applying Itô's lemma to (18), we obtain

$$dV = \frac{1}{\Gamma(1+\alpha)}\frac{\partial^{\alpha}V}{\partial t^{\alpha}}(dt)^{\alpha} + rX\frac{\partial V}{\partial X}\,dt + \frac{1}{2}\sigma^2X^2\frac{\partial^2 V}{\partial X^2}(dt)^{\alpha}. \tag{21}$$

Using the conversion formula (17) for dt, we replace dt in equation (21) with its equivalent expression:

$$dt = t^{1-\alpha}(dt)^{\alpha}\frac{1}{\Gamma(1+\alpha)\Gamma(2-\alpha)} \tag{22}$$

which implies that

$$dV = \frac{1}{\Gamma(1+\alpha)}\frac{\partial^{\alpha}V}{\partial t^{\alpha}}(dt)^{\alpha} + r\frac{Xt^{1-\alpha}}{\Gamma(1+\alpha)\Gamma(2-\alpha)}\frac{\partial V}{\partial X}(dt)^{\alpha} + \frac{1}{2}\sigma^2X^2\frac{\partial^2 V}{\partial X^2}(dt)^{\alpha}. \tag{23}$$

Finally, multiplying both sides of equation (23) by $\Gamma(1+\alpha)$ and simplifying the terms from relations (16) to (18), we obtain the time-fractional Black-Scholes PDE

$$\frac{\partial^\alpha V}{\partial t^\alpha} = \left(rV - rX\frac{\partial V}{\partial X}\right)\frac{t^{1-\alpha}}{\Gamma(2-\alpha)} - \frac{\Gamma(1+\alpha)}{2}\sigma^2 X^2 \frac{\partial^2 V}{\partial X^2}, \quad \text{where } 0<\alpha\leq 1 \tag{24}$$

By introducing the change of variable $\tau = T - t$ and incorporating the specified boundary conditions, we assert that (24) can be transformed as follows:

$$\begin{cases} \dfrac{\partial^\alpha V}{\partial \tau^\alpha} = \left[rV - rX\dfrac{\partial V}{\partial X}\right]\dfrac{\tau^{1-\alpha}}{\Gamma(2-\alpha)} - \dfrac{\Gamma(1+\alpha)\tau^{1-\alpha}}{2(T-\tau)^{1-\alpha}}\sigma^2 X^2 \dfrac{\partial^2 V}{\partial X^2}, \quad X^*(\tau)\leq X\leq\infty, \text{ and } \tau\in[0, T], \\ V(X, T) = \max\{E-X, 0\}, \text{ for } X\geq 0, \\ \dfrac{\partial V}{\partial X}(X^*(\tau), \tau) = -1, \\ V(X^*(\tau), \tau) = E - X^*(\tau), \\ \lim\limits_{X\to\infty} V(X, T) = 0, \\ X^*(T) = E, \\ V(X(\tau), \tau) = E - X, \text{ for } X\in[0, X^*(\tau)) \end{cases} \tag{25}$$

Where $\tau = T - t$ represents the period until maturity T, $X^*(t)$ unknown early exercise-free boundary with $X^*(t) > 0$, E is strike price, T expiration time, σ volatility and r the interest rate.

This model considers the America put option and it is only natural to define the arbitrage associated with it. For this purpose, we introduce the following subsection which explains the notion of arbitrage free corresponding to the model under consideration.

2.4 *Arbitrage-free pricing of American put options*

Ensuring arbitrage-free pricing of American put options requires adherence to two fundamental conditions: the value matching condition and the smooth pasting condition which both play a critical role in eliminating arbitrage opportunities and maintaining consistency within the financial market structure, we refer to the work in [44] for further investigation.

Note that the Value Matching condition, expressed as $V(X^*(\tau), \tau) = E - X^*(\tau)$ in the set up of the American put option, states that the price of the option must be equal to its intrinsic value at the optimal exercise boundary. To be more precise, we denote by $X^*(\tau)$ to be the optimal exercise boundary at time τ. This condition ensures that exercising the option does not produce profit beyond the guaranteed payoff $E - X^*(\tau)$. Thus far, this eliminating arbitrage opportunities. If violated, arbitrageurs could exploit pricing discrepancies by exercising the option and simultaneously trading the underlying asset to secure risk-free profits, see for instance the detailed expansion in [45].

Furthermore, the principle of put-call parity reinforces the necessity of this condition in preventing arbitrage, even in nonlinear pricing models where early exercise features complicate valuation [44] where the nonlinear pricing of put and call options in the financial market has been studied, [46] for instance where various mathematical models used in the financial market have been derived, and [28].

The smooth pasting condition, expressed as $\frac{\partial V}{\partial X}(X^*(\tau), \tau) = -1$ in the American put option framework, ensures that the option value function transitions smoothly across the early exercise boundary. This condition guarantees continuity in the slope of the value function $V(X^*(\tau), \tau) = E - X^*(\tau)$ and $\frac{\partial V}{\partial X}(X^*(\tau), \tau)$, preventing abrupt changes that could create arbitrage opportunities.

A discontinuity would allow sudden changes in the hedge ratio to be exploited to construct risk-free portfolios with guaranteed profits [47]. Furthermore, arbitrage-free pricing models highlight the crucial role of smooth pasting in ensuring a seamless transition between holding and exercising American options [28, 45, 46] which deals with the robust numerical scheme for solving the problem of the American put option using fractional partial differential equations of Black-Scholes types.

These conditions are fundamental because, in an arbitrage-free market, the transition between holding and exercising an option must occur smoothly, without introducing price discontinuities or abrupt shifts in the hedging strategy. A violation of the value matching condition would enable arbitrageurs to exploit pricing discrepancies by exercising the option and concurrently trading the underlying asset to generate risk-free profits, see the references for further description in this direction: [28, 46, 47].

At the optimal exercise boundary, an investor must decide whether to continue holding the option or exercising it with immediate effect. The value matching condition ensures that exercising does not create unaccounted excess value, while the smooth pasting condition guarantees a seamless transition, preventing exploitable pricing discontinuities. Together, these conditions ensure that the optimal stopping problem defining $X^*(\tau)$ is well-posed within the framework of the variational inequality governing the pricing of American options, see e.g., the work in the papers [28, 46, 48] where further details can be found in the references therein.

A key feature of American-style derivatives is their flexibility, allowing early exercise at any time before expiration, unlike European options. This flexibility requires that portfolio adjustments associated with early exercise remain self-financing, meaning that the reallocation of wealth between the option and the underlying asset should not require external capital infusion. Mathematically, this is enforced by the free-boundary problem in the price of American options, where $X^*(\tau)$ must be determined in conjunction with the PDE governing the value of the option $V(X, \tau)$.

Since early exercise involves liquidating the option in exchange for cash while simultaneously taking a short position in the underlying asset, any misalignment between the option's value and its intrinsic value would create arbitrage opportunities. Therefore, the value matching and smooth pasting conditions eliminate such possibilities by ensuring that transactions along the free boundary conditions satisfy the self-financing constraint. This ensures that each trade at $X = X^*(\tau)$ is precisely covered by the cash flows generated from either exercising or holding the option, for instance the manuscripts [28, 46, 48] for further subsequent development in this direction.

3. The front-fixing method

Free boundary problems are inherently challenging due to the requirement of solving a Partial Differential Equation (PDE) that must satisfy initial and boundary conditions on both a fixed and an unknown free boundary. To manage this complexity, these problems are typically reformulated as nonlinear PDEs, treating the free boundary as an unknown variable. A prominent method to address this is the front-fixing method, which transforms the original PDE into a new nonlinear PDE within a bounded domain, facilitating direct computation of the free boundary.

The front-fixing method, grounded in physics and based on the Landau transformation, simplifies the problem by "fixing" the unknown boundary along a vertical axis. This transformation enables a more manageable analysis. The front-fixing approach has been widely applied across disciplines such as physics and finance, including but not limited to option pricing, the method was initially introduced by Wu and Kwok [46] in 1997 for financial applications. Since then, it has been refined by researchers such as Riccardo et al. [1, 49], Company et al. [15], Nielsen [50], Ševčovič [51], and Zhang and Zhu [52], among others.

A key advantage of the front-fixing method is its capacity to directly compute the free boundary, which is crucial for analyzing the system's behavior. For instance, in the context of the Black-Scholes equation for American put options, the problem is transformed into a parabolic equation within a bounded domain, where a truncated boundary is introduced, and finite-difference schemes are applied to solve the resulting approximate problem.

Whenever $X \leq X^*(\tau)$, it is optimal to exercise the put option, while for $X^*(\tau) < X$, the optimal strategy is to hold the option, since exercising it under these conditions is not financially viable. The value-matching condition $v(X^*(\tau), \tau) = E - X^*(\tau)$ and the smooth-pasting condition $\frac{\partial v}{\partial X}(X^*(\tau), \tau) = -1$ are essential to maintaining the financial interpretation of the continuity of v and $\frac{\partial v}{\partial X}$ across the optimal exercise boundary $X^*(\tau)$. These conditions prevent arbitrage opportunities, ensuring that transactions are self-financing meaning that each portfolio adjustment is precisely funded by the proceeds from the previous position's sale.

3.1 *Derivation of the transformed fractional PDE*

The front-fixing method addresses the moving exercise boundary $X^*(\tau)$ by introducing a change of variables, converting the problem into a nonlinear time-fractional Black-Scholes PDE (tfBS-PDE) defined over a fixed domain. This transformation allows for a given boundary position while some boundary conditions remain unknown and must be computed simultaneously with the option value. For numerical implementation, the following change of variables (dimensionless variables), similar to [1, 2, 18], is considered:

- Logarithmic scale for stock price: $y = \ln\left(\frac{X}{X_f(\tau)}\right)$, where $X_f(\tau)$ is a time-dependent scaling factor.
- New dependent variable: $v(y, t) = \frac{V(X, \tau)}{K}$, where $K > 0$ is a constant.
- Scaling for $X_f(\tau) : X_f(\tau) = \frac{X^*(\tau)}{K}$.

Arguing similarly as in [20], and applying the Landau transformation, $y = \ln\left(\frac{X}{X_f(\tau)}\right)$ to the asset price variable ensures that $y = 0$ whenever $X = X^*(\tau)$. Therefore, this help converting the free boundary condition into a fixed boundary condition. Consequently, the stock dynamics is modified as follows:

$$dy = \left(r - \frac{\sigma^2}{2} - \frac{X_f'(\tau)}{X_f(\tau)}\right) dt + \sigma\omega(t)(dt)^{\alpha/2}, \quad 0 < \alpha \leq 1 \tag{26}$$

Using transformations of (26) and the above change of variables, we can transform each part of (25) using new variables as given below.

The first derivative of $V(X, t)$ with respect to X is transformed as:

$$\frac{\partial V}{\partial X} = \frac{\partial}{\partial X}\left(v(y, \tau)\right) = \frac{\partial v}{\partial y}\frac{\partial y}{\partial X}$$

Using $y = \ln\left(\frac{X}{X_f(\tau)}\right)$, we can obtain

$$\frac{\partial y}{\partial X} = \frac{1}{X} \text{ and } X = e^y X_f(\tau)$$

which implies that

$$\frac{\partial V}{\partial X} = \frac{\partial v}{\partial y}\frac{1}{X} = \frac{1}{e^y X_f(\tau)}\frac{\partial v}{\partial y}.$$

Therefore

$$X\frac{\partial V}{\partial X} = \frac{\partial v}{\partial y}. \tag{27}$$

Next, we can transform the second derivative of $V(X, t)$ with respect to X using the chain rule. Similarly to the above transformation, we notice that the second derivative becomes

$$\frac{\partial^2 V}{\partial X^2} = \frac{\partial}{\partial X}\left(\frac{\partial v}{\partial y}\frac{\partial y}{\partial X}\right) = \frac{\partial^2 V}{\partial X^2} = \frac{\partial}{\partial X}\left(\frac{1}{e^y X_f(\tau)}\frac{\partial v}{\partial y}\right). \tag{28}$$

Taking the derivative with respect to X, and noting that

$$\frac{\partial y}{\partial X} = \frac{1}{X}$$

hence, we obtain

$$\frac{\partial^2 V}{\partial X^2} = \frac{1}{(X_f(\tau))^2 e^{2y}}\frac{\partial^2 v}{\partial y^2} = \frac{1}{X^2}\frac{\partial^2 v}{\partial y^2}. \tag{29}$$

Finally, we can transform the fractional time derivative of $V(X, \tau)$ with respect to τ. For this purpose, we apply the fractional time derivative $\dfrac{\partial^\alpha (V(X, \tau))}{\partial \tau^\alpha}$ and applying the chain rule we obtain that

$$\frac{\partial^\alpha V}{\partial \tau^\alpha} = \frac{\partial^\alpha v}{\partial \tau^\alpha} + \frac{\partial y}{\partial \tau} = \frac{\partial^\alpha v}{\partial \tau^\alpha} - \frac{X_f'(\tau)}{X_f(\tau)}\frac{\partial v}{\partial y}. \tag{30}$$

Now, using the previous change of variables, we can combine relations (27)-(30) with (25) and factor out the common terms, then after simplification, the transformed equation becomes

$$\frac{\partial^\alpha v}{\partial \tau^\alpha} = \phi(\tau)\left(\left(rv - \left(r - \frac{\sigma^2}{2}\right)\frac{\partial v}{\partial y}\right)\frac{(T-\tau)^{1-\alpha}}{\Gamma(2-\alpha)} + \frac{X_f'(\tau)}{X_f(\tau)}\frac{\partial v}{\partial y} - \frac{\Gamma(1+\alpha)\sigma^2}{2}\frac{\partial^2 v}{\partial x^2}\right) \tag{31}$$

where $\phi(\tau) = \tau^{1-\alpha}(T-\tau)^{\alpha-1}$ which represents the combined influence of past and future memory contributions inherent to fractional calculus. Similar development can be found in the papers by Nuugulu and his coauthors [28] and by Ali et al. [29, 40].

After simplifying equation (31), we obtain the tfBS-PDE, given in (25). This equation is expressed in terms of the newly introduced variable y, which facilitates a more efficient analysis of the problem. Thus far, the newly transformed fraction derivative of V can be written as:

$$\begin{cases} \dfrac{\partial^\alpha v}{\partial \tau^\alpha} = \theta(\tau)\left[rv - \left(r - \dfrac{\sigma^2}{2}\right)\dfrac{\partial v}{\partial y}\right] - \varphi(\tau)\dfrac{\sigma^2}{2}\dfrac{\partial^2 v}{\partial y^2} + \phi(\tau)\dfrac{X_f'(\tau)}{X_f(\tau)}\dfrac{\partial v}{\partial y} = 0 \\ \theta(\tau) = \dfrac{\tau^{1-\alpha}}{\Gamma(2-\alpha)},\ \varphi(\tau) = \dfrac{\Gamma(1+\alpha)\tau^{1-\alpha}}{(T-\tau)^{1-\alpha}},\ \phi(\tau) = \dfrac{\tau^{1-\alpha}}{(T-\tau)^{1-\alpha}}\ \ X^*(\tau) \leq X \leq \infty, \quad \text{and} \quad t \in [0, T], \\ v(0, y) = 0, \quad \text{for} \quad y \geq 0, X_f(0) = 1, \\ \lim\limits_{y \to \infty} v(\tau, y) = 0, \\ v(\tau, 0) = 1 - X_f(\tau),\ \dfrac{\partial v}{\partial y}(\tau, 0) = -X_f(\tau) \\ \text{on} \quad 0 \leq t \leq T \quad \text{and} \quad 0 \leq X(\tau) \leq X^*(\tau). \end{cases} \tag{32}$$

3.2 *Crank-Nicolson finite-difference scheme*

In this section, we define a numerical scheme to compute the grid values of APO. For this purpose, we start by truncating the interval $(0, \infty)$ into the new interval $(0, Y)$ which will help us to solve the problem. To determine the appropriate value of $Y = y_\infty$ and ensure the accuracy of the corresponding numerical solution, we adapt the methodology proposed by Kangro et al. [53] and Wilmott et al. [54], which has been successfully applied to solving the multidimensional Black-Scholes equation. Therefore, we obtain $v(t, Y) = 0$ from the boundary condition given by (32). In the rest of the paper, we shall solve the time Caputo-Fabrizio fractional differential equation of APO using the Crank-Nicolson finite-difference method. Namely, the problem can be studied on $(0, T] \times [0, Y]$ with $M \in \mathbb{N}$ and $\mu \in \mathbb{R}^+$. Having said that, we are now ready to set the step size as follows:

$$\begin{aligned} &\Delta y = \frac{Y}{M} \\ &\Delta \tau = \mu(\Delta y)^2 \\ &\text{The integer } N = \left\lceil \frac{T}{\Delta \tau} \right\rceil \end{aligned} \tag{33}$$

where $\lceil . \rceil : \mathscr{R}^+ \to \mathbb{N}$ is the ceiling function. Hence, the grid-ratio μ is then given by

$$\mu = \frac{\Delta \tau}{(\Delta y)^2}.$$

A mesh of grid points can be introduced in the finite domain as follows:

$$y_m = m\Delta y,$$

$$\tau^n = n\Delta\tau, \quad \text{for} \quad m = 0, 1, \ldots, M \quad \text{and} \quad n = 0, 1, \ldots, N.$$

To compute the grid values, we construct a numerical scheme, and the free boundary values by setting

$$v_m^n \approx v(\tau^n, y_m)$$

$$X_f^n = X_f(\tau^n), \quad \text{for } m = 0, 1, \ldots, M \text{ and } n = 0, 1, \ldots, N.$$

Having defined the size of the mesh of grid points concerning time and space which we can use to compute the numerical scheme of the grid value of APO, we will now progress to develop a new Crank-Nicolson finite-difference scheme of the considered APO. We can now present the Crank-Nicolson finite-difference scheme, which to the best of our knowledge has been investigated for the first time in this manuscript.

The Jumarie (6) and the new Caputo-Fabrizio fractional derivatives (2) are equivalent for differentiable functions, see e.g., [28] for a detailed investigation. Note that the fractional derivative of order α in (32) will be evaluated using (2). However, similar results can also be obtained whenever one replaces the fractional operator used here with the closely related operations apart from those discussed in the above definitions.

First, we discretize the terms in the fractional derivatives appearing in (32) using (2). We have

$$\begin{aligned}
\frac{\partial^\alpha v}{\partial \tau^\alpha} &= \frac{1}{(1-\alpha)} \int_0^{t_n} v'(\tau) e^{-\frac{\alpha(t_n-\tau)}{1-\alpha}} d\tau \\
&= \frac{1}{(1-\alpha)} \sum_{j=1}^{n} \int_{(j-1)k}^{jk} \left(\left(\frac{v_m^{j+1} - v_m^j}{\Delta\tau} \right) + \mathscr{O}(k) \right) e^{-\frac{\alpha(t_n-\tau)}{1-\alpha}} d\tau \\
&= \frac{1}{(1-\alpha)} \sum_{j=1}^{n} \int_{(j-1)k}^{jk} \left(\frac{1}{k}(v_m^{j+1} - v_m^j) + \mathscr{O}(k) \right) e^{-\frac{\alpha(nk-\tau)}{1-\alpha}} d\tau \\
&= \frac{1}{(1-\alpha)} \sum_{j=1}^{n} \left(\frac{1}{k}(v_m^{j+1} - v_m^j) + \mathscr{O}(k) \right) \frac{(1-\alpha)}{\alpha} \int_{(j-1)k}^{jk} e^{-\frac{\alpha(nk-\tau)}{1-\alpha}} d\tau \\
&= \frac{1}{k\alpha} \sum_{j=1}^{n} \left((v_m^{j+1} - v_m^j) + \mathscr{O}(k) \right) \left(e^{-\frac{\alpha(n-j)k}{1-\alpha}} - e^{-\frac{\alpha(n+1-j)k}{1-\alpha}} \right).
\end{aligned}$$

Shifting the indices in the above equation yields

$$= \frac{1}{k\alpha}\sum_{j=1}^{n}\left((v_m^{n-j+1} - v_m^{n-j}) + \mathscr{O}(k)\right)\left(e^{-\frac{\alpha jk}{1-\alpha}} - e^{-\frac{\alpha(j+1)k}{1-\alpha}}\right)$$

$$= \frac{1}{k\alpha}\left(1 - e^{-\frac{\alpha k}{1-\alpha}}\right)\sum_{j=1}^{n}\left((v_m^{n-j+1} - v_m^{n-j}) + \mathscr{O}(k)\right)e^{-\frac{\alpha jk}{1-\alpha}}$$

$$= \beta\sum_{j=1}^{n}(v_m^{n-j+1} - v_m^{n-j})e^{-\frac{\alpha jk}{1-\alpha}} + \mathscr{O}(k)\frac{1}{k\alpha}(1 - e^{-\frac{\alpha k}{1-\alpha}})$$

$$= \beta\sum_{j=1}^{n}(v_m^{n-j+1} - v_m^{n-j})e^{-\frac{\alpha jk}{1-\alpha}} + \mathscr{O}(1) \tag{34}$$

where

$$\beta = \frac{1}{k\alpha}(1 - e^{-\frac{\alpha k}{1-\alpha}}).$$

Using the above equation (34) we can literally analyze each term in it as follows:

$$\mathscr{O}(k)\frac{1}{k\alpha}(1 - e^{-\frac{\alpha k}{1-\alpha}}).$$

First, we deal with the following term:

$$\frac{O(k)}{k\alpha}$$

where

- $O(k)$: represents the growth proportional to k, potentially with smaller terms.
- $k\alpha$: grows linearly in k since α is constant.

Hence,

$$\frac{O(k)}{k\alpha} \approx \frac{D}{\alpha},$$

where D is the constant obtained from the expression of $O(k)$.

Next we will analyze the order of

$$1 - e^{-\frac{\alpha k}{1-\alpha}}.$$

Since $0 < \alpha < 1$, the exponent $-\dfrac{\alpha k}{1-\alpha}$ becomes extremely small as $k \to \infty$. Therefore,

$$e^{-\frac{\alpha k}{1-\alpha}} \to 0, \quad \text{and} \quad 1 - e^{-\frac{\alpha k}{1-\alpha}} \to 1 \quad \text{as} \quad k \to \infty.$$

Finally, we obtain

$$\frac{O(k)}{k\alpha} \cdot 1 \approx \frac{D}{\alpha}.$$

Since the right hand side is independent of k, then we can literally assert that the error order is $O(1)$.

Subsequently, the Crank-Nicolson scheme can be used to discretize the derivative terms on the the right-hand side the fractional derivative terms appearing in (32). Then we can now obtain

$$rv = \frac{rv_m^{n+1} + rv_m^n}{2}$$

$$\frac{\partial v}{\partial y} = \frac{1}{2}\left(\frac{v_{m+1}^{n+1} - v_{m-1}^{n+1}}{2\Delta y} + \frac{v_{m+1}^{n} - v_{m-1}^{n}}{2\Delta y}\right)$$

$$\frac{\partial^2 v}{\partial y^2} = \frac{1}{2}\left(\frac{v_{m-1}^{n+1} - 2v_m^{n+1} + v_{m+1}^{n+1}}{\Delta y^2} + \frac{v_{m-1}^{n} - 2v_m^{n} + v_{m+1}^{n}}{\Delta y^2}\right)$$

$$\frac{1}{X_f^n}\frac{dX_f^n}{d\tau}\frac{\partial v}{\partial y} = \frac{1}{2X_f^n}\frac{X_f^{n+1} - X_f^n}{(\Delta\tau)}\left(\frac{v_{m+1}^{n+1} - v_{m-1}^{n+1}}{2\Delta y} + \frac{v_{m+1}^{n} - v_{m-1}^{n}}{2\Delta y}\right)$$

$$\text{for } m = 1, 2, \ldots, M-1 \text{ and } n = 1, 2, \ldots, N. \tag{35}$$

By combining equations (34) and (35) we can obtain a new Crank-Nicolson finite-difference (time-discretization) scheme for internal special nodes given by the following:

$$\begin{aligned} 2\beta \sum_{j=1}^{n} (v_m^{n-j+1} - v_m^{n-j}) e^{-\frac{\alpha jk}{1-\alpha}} &= \theta\left(\tau^{n+1}\right)\left[(rv_m^{n+1} + rv_m^n) - \left(r - \frac{\sigma^2}{2}\right)\left(\frac{v_{m+1}^{n+1} - v_{m-1}^{n+1}}{2\Delta y} + \frac{v_{m+1}^{n} - v_{m-1}^{n}}{2\Delta y}\right)\right] \\ &\quad - \varphi(\tau^{n+1})\frac{\sigma^2}{2}\left(\frac{v_{m-1}^{n+1} - 2v_m^{n+1} + v_{m+1}^{n+1}}{\Delta y^2} + \frac{v_{m-1}^{n} - 2v_m^{n} + v_{m+1}^{n}}{\Delta y^2}\right) \\ &\quad + \frac{\phi(\tau^{n+1})}{X_f^n}\frac{X_f^{n+1} - X_f^n}{(\Delta\tau)}\left(\frac{v_{m+1}^{n+1} - v_{m-1}^{n+1}}{2\Delta y} + \frac{v_{m+1}^{n} - v_{m-1}^{n}}{2\Delta y}\right) \end{aligned} \tag{36}$$

After collecting all like terms, we obtain the following expression:

$$
\begin{aligned}
&-2\beta\sum_{j=1}^{n}(v_m^{n-j+1}-v_m^{n-j})e^{-\frac{\alpha jk}{1-\alpha}}\\
&+v_{m+1}^{n+1}\left[\frac{-\theta(\tau^{n+1})\left(r-\dfrac{\sigma^2}{2}\right)}{2\Delta y}-\varphi(\tau^{n+1})\frac{\sigma^2}{2\Delta y^2}+\frac{\phi(\tau^{n+1})}{X_f^n}\frac{X_f^{n+1}-X_f^n}{2\Delta y\Delta\tau}\right]\\
&+v_{m+1}^{n}\left[\frac{-\theta(\tau^{n+1})\left(r-\dfrac{\sigma^2}{2}\right)}{2\Delta y}-\varphi(\tau^{n+1})\frac{\sigma^2}{2\Delta y^2}+\frac{\phi(\tau^{n+1})}{X_f^n}\frac{X_f^{n+1}-X_f^n}{2\Delta y\Delta\tau}\right]\\
&+v_{m-1}^{n+1}\left[\frac{\theta(\tau^{n+1})\left(r-\dfrac{\sigma^2}{2}\right)}{2\Delta y}-\varphi(\tau^{n+1})\frac{\sigma^2}{2\Delta y^2}-\frac{\phi(\tau^{n+1})}{X_f^n}\frac{X_f^{n+1}-X_f^n}{2\Delta y\Delta\tau}\right]\\
&+v_{m-1}^{n}\left[\frac{\theta(\tau^{n+1})\left(r-\dfrac{\sigma^2}{2}\right)}{2\Delta y}-\varphi(\tau^{n+1})\frac{\sigma^2}{2\Delta y^2}-\frac{\phi(\tau^{n+1})}{X_f^n}\frac{X_f^{n+1}-X_f^n}{2\Delta y\Delta\tau}\right]\\
&+v_m^{n+1}\left[\theta(\tau^{n+1})r+\varphi(\tau^{n+1})\frac{\sigma^2}{\Delta y^2}\right]+v_m^{n}\left[\theta(\tau^{n+1})r+\varphi(\tau^{n+1})\frac{\sigma^2}{\Delta y^2}\right]=0.
\end{aligned}
\tag{37}
$$

Our Crank-Nicolson numerical scheme (37) can be rewritten as

$$
\begin{aligned}
&\bar{A}^{n+1}v_{m+1}^{n+1}+\bar{B}^{n+1}v_{m-1}^{n+1}+\bar{C}^{n+1}v_m^{n+1}+\bar{A}^{n+1}v_{m+1}^{n}+\bar{B}^{n+1}v_{m-1}^{n}+\bar{C}^{n+1}v_m^{n}\\
&-2\beta\sum_{j=1}^{n}(v_m^{n-j+1}-v_m^{n-j})e^{-\frac{\alpha jk}{1-\alpha}}=0
\end{aligned}
$$

which can be reduced to obtain the new scheme:

$$
\begin{aligned}
v_{m+1}^{n+1}=&-(\bar{B}^{n+1}/\bar{A}^{n+1})v_{m-1}^{n+1}-(\bar{C}^{n+1}/\bar{A}^{n+1})v_m^{n+1}-(\bar{A}^{n+1}/\bar{A}^{n+1})v_{m+1}^{n}-(\bar{B}^{n+1}/\bar{A}^{n+1})v_{m-1}^{n}-(\bar{C}^{n+1}/\bar{A}^{n+1})v_m^{n}\\
&+(2\beta/\bar{A}^{n+1})\sum_{j=1}^{n}(v_m^{n-j+1}-v_m^{n-j})e^{-\frac{\alpha jk}{1-\alpha}}\quad\text{for}\quad m=1,2,\ldots,M-1\quad\text{and}\quad n=1,\ldots,N
\end{aligned}
\tag{38}
$$

where

$$\bar{A}^{n+1}=\frac{-\theta(\tau^{n+1})\left(r-\dfrac{\sigma^2}{2}\right)}{2\Delta y}-\varphi(\tau^{n+1})\frac{\sigma^2}{2\Delta y^2}+\frac{\phi(\tau^{n+1})}{X_f^n}\frac{X_f^{n+1}-X_f^n}{2\Delta y\Delta\tau}$$

$$\bar{B}^{n+1}=\frac{\theta(\tau^{n+1})\left(r-\dfrac{\sigma^2}{2}\right)}{2\Delta y}-\varphi(\tau^{n+1})\frac{\sigma^2}{2\Delta y^2}-\frac{\phi(\tau^{n+1})}{X_f^n}\frac{X_f^{n+1}-X_f^n}{2\Delta y\Delta\tau}$$

$$\bar{C}^{n+1}=\theta(\tau^{n+1})r+\varphi(\tau^{n+1})\frac{\sigma^2}{\Delta y^2}. \tag{39}$$

It follows from the initial and boundary conditions in (32) that

$$\begin{cases} v_0^n=1-X_f^n, & \text{for } n=0,\,1,\,\ldots,\,N \\ \dfrac{\partial v}{\partial y}(\tau,\,0)=-X_f^n(\tau), & \\ v_m^0=0, & \text{for } m=0,\,1,\,\ldots,\,M \\ X_f^0=1, & \text{for } m=0,\,1,\,\ldots,\,M \\ v_M^n=0, & \text{for } n=0,\,1,\,\ldots,\,N. \end{cases} \tag{40}$$

To present and validate equation (38) in matrix form, we intend in using an induction technique. To illustrate this, we start with the initial case $n=1$, yielding:

$$\bar{A}^2v_{m+1}^2+\bar{B}^2v_{m-1}^2+\bar{C}^2v_m^2+\bar{A}^2v_{m+1}^1+\bar{B}^2v_{m-1}^1+\bar{C}^2v_m^1-2\beta(v_m^1-v_m^0)e^{-\frac{\alpha k}{1-\alpha}}=0$$

from which we infer that

$$\bar{A}^2v_{m+1}^2+\bar{B}^2v_{m-1}^2+\bar{C}^2v_m^2=-\bar{B}^2v_{m-1}^1-\bar{A}^2v_{m+1}^1-\bar{C}^2v_m^1+2\beta v_m^1e^{-\frac{\alpha k}{1-\alpha}}. \tag{41}$$

For $n=2$, we have

$$\bar{A}^3v_{m+1}^3+\bar{B}^3v_{m-1}^3+\bar{C}^3v_m^3+\bar{A}^3v_{m+1}^2+\bar{B}^3v_{m-1}^2+\bar{C}^3v_m^2-2\beta\sum_{j=1}^{2}(v_m^{n-j+1}-v_m^{n-j})e^{-\frac{\alpha jk}{1-\alpha}}=0 \tag{42}$$

from which we infer that

$$\bar{A}^3 v_{m+1}^3 + \bar{B}^3 v_{m-1}^3 + \bar{C}^3 v_m^3 = -\bar{A}^3 v_{m+1}^2 - \bar{B}^3 v_{m-1}^2 - \bar{C}^3 v_m^2 + 2\beta \sum_{j=1}^{2} (v_m^{n-j+1} - v_m^{n-j}) e^{-\frac{\alpha jk}{1-\alpha}}. \tag{43}$$

Similarly, we obtain for $n >= 3$ the following result

$$\bar{A}^{n+1} v_{m+1}^{n+1} + \bar{B}^{n+1} v_{m-1}^{n+1} + \bar{C}^{n+1} v_m^{n+1} = -\bar{A}^{n+1} v_{m+1}^n - \bar{B}^{n+1} v_{m-1}^n - \bar{C}^{n+1} v_m^n + 2\beta \sum_{j=1}^{n} (v_m^{n-j+1} - v_m^{n-j}) e^{-\frac{\alpha jk}{1-\alpha}}. \tag{44}$$

At each time step, we obtain a system of linear equations with $M-1$ variables and $M+1$ equations. These equations are valid for $m = 1, 2, 3\ldots, M-1$, while the boundary conditions provide the additional two equations needed. The system can now be expressed in matrix form as follows

$$\begin{bmatrix} B^1 & C^1 & A^1 & & 0\ldots & \ldots & \ldots & \ldots \\ 0 & B^2 & C^2 & A^2 & 0\ldots & \ldots & \ldots & \ldots \\ 0 & 0 & B^3 & C^3 & A^3 & 0 & \ldots & \ldots \\ 0 & 0 & 0 & B^4 & C^4 & A^4 & 0\ldots & \\ \vdots & \vdots & \vdots & \vdots & \vdots & \ddots & \ddots & \ddots \\ 0 & 0 & 0 & 0 & 0 & 0 & 0 & B^{n+1} \end{bmatrix} \times \begin{bmatrix} v_0^{n+1} \\ v_1^{n+1} \\ v_2^{n+1} \\ \vdots \\ \vdots \\ v_M^{n+1} \end{bmatrix}$$

$$= \begin{bmatrix} B^1 & C^1 & A^1 & & 0\ldots & \ldots & \ldots & \ldots \\ 0 & B^2 & C^2 & A^2 & 0\ldots & \ldots & \ldots & \ldots \\ 0 & 0 & B^3 & C^3 & A^3 & 0 & \ldots & \ldots \\ 0 & 0 & 0 & B^4 & C^4 & A^4 & 0\ldots & \\ \vdots & \vdots & \vdots & \vdots & \vdots & \ddots & \ddots & \ddots \\ 0 & 0 & 0 & 0 & 0 & 0 & 0 & B^{n+1} \end{bmatrix} \times \begin{bmatrix} v_0^{n} \\ v_1^{n} \\ v_2^{n} \\ \vdots \\ \vdots \\ v_M^{n} \end{bmatrix}$$

$$+ \begin{bmatrix} v_0^0 \\ 2\beta \sum_{j=1}^n (v_m^{n-j+1} - v_m^{n-j}) e^{-\frac{\alpha jk}{1-\alpha}} \\ 2\beta \sum_{j=1}^n (v_m^{n-j+1} - v_m^{n-j}) e^{-\frac{\alpha jk}{1-\alpha}} \\ 2\beta \sum_{j=1}^n (v_m^{n-j+1} - v_m^{n-j}) e^{-\frac{\alpha jk}{1-\alpha}} \\ 2\beta \sum_{j=1}^n (v_m^{n-j+1} - v_m^{n-j}) e^{-\frac{\alpha jk}{1-\alpha}} \\ \vdots \\ 2\beta \sum_{j=1}^n (v_m^{n-j+1} - v_m^{n-j}) e^{-\frac{\alpha jk}{1-\alpha}} \end{bmatrix}. \tag{45}$$

The matrix structure described above consists of $M-1$ rows and $M+1$ columns, aligned with the $M-1$ interior points and the $M+1$ unknowns. Note that the variables v_{N+1}^{-1} and v_{N+1}^{M+1} fall outside the computational domain. To address this challenge, we derive two additional equations from the boundary conditions, allowing us to reformulate the system as one with square matrices where boundary constraints are fully integrated. We must emphasize that in order for us to incorporate the boundary conditions, we use the vanishing term: $v_{N+1}^{M+1} = 0$, which allows us to start the boundary application at $m = 0$. Furthermore, substituting the boundary condition of (32) into the main fractional differential equation that can be seen at the start of the same equations in (32) at $m = 0$ yields the following modified boundary condition:

$$\frac{\partial^{\alpha}(v_0^{n+1})}{\partial t^{\alpha}} = \theta(\tau^{n+1})\left[r(1-X_f)+\left(r-\frac{\sigma^2}{2}\right)X_f\right]-\varphi(\tau^{n+1})\frac{\sigma^2}{2}\frac{\partial^2 v}{\partial y^2}+\frac{\phi(\tau^{n+1})}{X_f(\tau)}\frac{dX_f(\tau)}{d\tau}\frac{\partial v}{\partial y}=0. \tag{46}$$

Now, we deduce the discretization of (46) as follows:

$$\begin{aligned}
&\beta\sum_{j=1}^{n}(-X^{n-j+1}+X^{n-j})e^{-\frac{\alpha jk}{1-\alpha}} \\
&= \theta(\tau^{n+1})\left[r-\frac{\sigma^2}{2}X_f^n\right]-\varphi(\tau^{n+1})\frac{\sigma^2}{4}\left(\frac{v_{-1}^{n+1}-2v_0^{n+1}+v_1^{n+1}}{\Delta y^2}+\frac{v_{-1}^{n}-2v_0^{n}+v_1^{n}}{\Delta y^2}\right) \\
&-\phi(\tau^{n+1})\frac{X_f^{n+1}-X_f^n}{\Delta\tau}.
\end{aligned} \tag{47}$$

It follows from the boundary conditions in (32) that

$$\begin{aligned}
&\frac{1}{4}\left(\frac{v_1^{n+1}-v_{-1}^{n+1}}{\Delta y}+\frac{v_1^{n}-v_{-1}^{n}}{\Delta y}\right)=-\frac{1}{2}(X_f^{n+1}(\tau)+X_f^n(\tau)); \\
&v_{-1}^{n+1}+v_{-1}^{n}=v_1^{n+1}+v_1^n+2(X_f^{n+1}(\tau)+X_f^n(\tau)); \\
&v_0^n = 1-X_f^n(\tau).
\end{aligned} \tag{48}$$

Now, inserting the boundary conditions (48) into (47) and then we obtain after easy simplification that

$$\begin{aligned}
&\beta\sum_{j=1}^{n}(X^{n-j+1}-X^{n-j})e^{-\frac{\alpha jk}{1-\alpha}}+\theta(\tau^{n+1})\left[r-\frac{\sigma^2}{2}X_f^n\right]-\phi(\tau^{n+1})\frac{X_f^{n+1}-X_f^n}{\Delta\tau} \\
&-\varphi(\tau^{n+1})\frac{\sigma^2}{4}\left(\frac{v_{-1}^{n+1}-2v_0^{n+1}+v_1^{n+1}+v_{-1}^{n}-2v_0^{n}+v_1^{n}}{\Delta y^2}\right)=0
\end{aligned}$$

which implies that

$$\beta\sum_{j=1}^{n}(X^{n-j+1}-X^{n-j})e^{-\frac{\alpha jk}{1-\alpha}}+\theta(\tau^{n+1})\left[r-\frac{\sigma^2}{2}X_f^n\right]-\phi(\tau^{n+1})\frac{X_f^{n+1}-X_f^n}{\Delta\tau}$$

$$-\varphi(\tau^{n+1})\frac{\sigma^2}{4}\left(\frac{2X^{n+1}\Delta y+2v_1^{n+1}-2(1-X^{n+1})+2X^n\Delta y+2v_1^n-2(1-X^n)}{\Delta y^2}\right)=0$$

from which we infer that

$$\beta\sum_{j=1}^{n}(X^{n-j+1}-X^{n-j})e^{-\frac{\alpha jk}{1-\alpha}}+\theta(\tau^{n+1})\left[r-\frac{\sigma^2}{2}X_f^n\right]-\phi(\tau^{n+1})\frac{X_f^{n+1}-X_f^n}{\Delta\tau}$$

$$-\varphi(\tau^{n+1})\frac{\sigma^2}{2}\left(\frac{(X^{n+1}+X^n)\Delta y+v_1^{n+1}+v_1^n-(1-X^{n+1})-(1-X^n)}{\Delta y^2}\right)=0.$$

This enables us to deduce that

$$\frac{2\Delta y^2}{\varphi(\tau^{n+1})\sigma^2}\left(\beta\sum_{j=1}^{n}(X^{n-j+1}-X^{n-j})e^{-\frac{\alpha jk}{1-\alpha}}+\theta(\tau^{n+1})\left[r-\frac{\sigma^2}{2}X_f^n\right]-\phi(\tau^{n+1})\frac{X_f^{n+1}-X_f^n}{\Delta\tau}\right)$$

$$=(X^{n+1}+X^n)(1+\Delta y)+v_1^{n+1}+v_1^n-2.$$

After simplifying the equation above, we obtain

$$v_1^{n+1}=\frac{2\Delta y^2}{\varphi(\tau^{n+1})\sigma^2}\left[\beta\sum_{j=1}^{n}(X^{n-j+1}-X^{n-j})e^{-\frac{\alpha jk}{1-\alpha}}+\theta(\tau^{n+1})\left[r-\frac{\sigma^2}{2}X_f^n\right]\right.$$

$$\left.-\phi(\tau^{n+1})\frac{X_f^{n+1}-X_f^n}{\Delta\tau}\right]-(X^{n+1}+X^n)(1+\Delta y)-v_1^n+2. \tag{49}$$

Combining all the above equations from (38) to (49), we deduce that

$$\mathbf{W_{n+1}v_{n+1}}+\mathbf{R_{n+1}}=\mathbf{W_n v_n}+\mathbf{L_n}+\Sigma_{n+1} \tag{50}$$

where

$$\mathbf{W_n} = \mathbf{W_{n+1}} \begin{bmatrix} C^1 & A^1 & & 0\dots & \dots & \dots & \dots & \\ 0 & B^2 & C^2 & A^2 & 0\dots & \dots & \dots & \dots \\ 0 & 0 & B^3 & C^3 & A^3 & 0 & \dots & \dots \\ 0 & 0 & 0 & B^4 & C^4 & A^4 & 0\dots & \\ \vdots & \vdots & \vdots & \vdots & \vdots & \ddots & \ddots & \ddots \\ 0 & 0 & 0 & 0 & 0 & 0 & B^{n+1} & C^{n+1} \end{bmatrix};$$

$$\mathbf{v^n} = \begin{bmatrix} v_1^n \\ v_2^n \\ \vdots \\ \vdots \\ v_{M-1}^n \end{bmatrix}; \mathbf{v^{n+1}} = \begin{bmatrix} v_1^{n+1} \\ v_2^{n+1} \\ \vdots \\ \vdots \\ v_{M-1}^{n+1} \end{bmatrix}; \mathbf{L^n} = \begin{bmatrix} B^n v_0^n \\ 0 \\ 0 \\ \vdots \\ \vdots \\ B^n v_M^n \end{bmatrix}; \mathbf{R^{n+1}} = \begin{bmatrix} B^{n+1} v_0^{n+1} \\ 0 \\ 0 \\ \vdots \\ \vdots \\ B^{n+1} v_M^{n+1} \end{bmatrix};$$

$$\Sigma_{n+1} = \begin{bmatrix} 2\beta \sum_{j=1}^{n} (v_m^{n-j+1} - v_m^{n-j}) e^{-\frac{\alpha jk}{1-\alpha}} \\ 2\beta \sum_{j=1}^{n} (v_m^{n-j+1} - v_m^{n-j}) e^{-\frac{\alpha jk}{1-\alpha}} \\ 2\beta \sum_{j=1}^{n} (v_m^{n-j+1} - v_m^{n-j}) e^{-\frac{\alpha jk}{1-\alpha}} \\ 2\beta \sum_{j=1}^{n} (v_m^{n-j+1} - v_m^{n-j}) e^{-\frac{\alpha jk}{1-\alpha}} \\ \vdots \\ 2\beta \sum_{j=1}^{n} (v_m^{n-j+1} - v_m^{n-j}) e^{-\frac{\alpha jk}{1-\alpha}} \end{bmatrix}.$$

Hence (50) becomes

$$\mathbf{v_{n+1}} = \mathbf{W_{n+1}^{-1}} (\mathbf{W_n} \mathbf{v_n} + \mathbf{L_n} + \Sigma_{n+1} - \mathbf{R_{n+1}}). \tag{51}$$

The Crank-Nicolson discretization of APO leads to the nonlinear equation (51) regarding the price and the free boundary conditions at each time step.

Now, to determine the value of X_f^n, we apply the schemes (37) and (49) at $m = 1$ and evaluate the time level n^{th} of the free boundary. Therefore,

$$v_2^{n+1} \left[\frac{-\theta(\tau^{n+1}) \left(r - \frac{\sigma^2}{2} \right)}{2\Delta y} - \varphi(\tau^{n+1}) \frac{\sigma^2}{2\Delta y^2} + \frac{\phi(\tau^{n+1})}{X_f^n} \frac{X_f^{n+1} - X_f^n}{2\Delta y \Delta \tau} \right]$$

$$+ v_2^n \left[\frac{-\theta(\tau^{n+1}) \left(r - \dfrac{\sigma^2}{2} \right)}{2\Delta y} - \varphi(\tau^{n+1}) \frac{\sigma^2}{2\Delta y^2} + \frac{\phi(\tau^{n+1})}{X_f^n} \frac{X_f^{n+1} - X_f^n}{2\Delta y \Delta \tau} \right]$$

$$+ v_0^{n+1} \left[\frac{\theta(\tau^{n+1}) \left(r - \dfrac{\sigma^2}{2} \right)}{2\Delta y} - \varphi(\tau^{n+1}) \frac{\sigma^2}{2\Delta y^2} - \frac{\phi(\tau^{n+1})}{X_f^n} \frac{X_f^{n+1} - X_f^n}{2\Delta y \Delta \tau} \right]$$

$$+ v_0^n \left[\frac{\theta(\tau^{n+1}) \left(r - \dfrac{\sigma^2}{2} \right)}{2\Delta y} - \varphi(\tau^{n+1}) \frac{\sigma^2}{2\Delta y^2} - \frac{\phi(\tau^{n+1})}{X_f^n} \frac{X_f^{n+1} - X_f^n}{2\Delta y \Delta \tau} \right]$$

$$+ v_1^{n+1} \left[\theta(\tau^{n+1}) r + \varphi(\tau^{n+1}) \frac{\sigma^2}{\Delta y^2} \right] + v_1^n \left[\theta(\tau^{n+1}) r + \varphi(\tau^{n+1}) \frac{\sigma^2}{\Delta y^2} \right]$$

$$- 2\beta \sum_{j=1}^{n} (v_1^{n+1} - v_1^n) e^{\frac{-\alpha jk}{1-\alpha}} = 0. \tag{52}$$

By incorporating v_0^n from equation (40) and v_1^n from equation (49) into equation (52), we derive the following result:

$$v_2^{n+1} \left[\frac{-\theta(\tau^{n+1}) \left(r - \dfrac{\sigma^2}{2} \right)}{2\Delta y} - \varphi(\tau^{n+1}) \frac{\sigma^2}{2\Delta y^2} + \frac{\phi(\tau^{n+1})}{X_f^n} \frac{X_f^{n+1} - X_f^n}{2\Delta y \Delta \tau} \right]$$

$$+ v_2^n \left[\frac{-\theta(\tau^{n+1}) \left(r - \dfrac{\sigma^2}{2} \right)}{2\Delta y} - \varphi(\tau^{n+1}) \frac{\sigma^2}{2\Delta y^2} + \frac{\phi(\tau^{n+1})}{X_f^n} \frac{X_f^{n+1} - X_f^n}{2\Delta y \Delta \tau} \right]$$

$$+ (1 - X_f^{n+1}) \left[\frac{\theta(\tau^{n+1}) \left(r - \dfrac{\sigma^2}{2} \right)}{2\Delta y} - \varphi(\tau^{n+1}) \frac{\sigma^2}{2\Delta y^2} - \frac{\phi(\tau^{n+1})}{X_f^n} \frac{X_f^{n+1} - X_f^n}{2\Delta y \Delta \tau} \right]$$

$$+ (1 - X_f^n) \left[\frac{\theta(\tau^{n+1}) \left(r - \dfrac{\sigma^2}{2} \right)}{2\Delta y} - \varphi(\tau^{n+1}) \frac{\sigma^2}{2\Delta y^2} - \frac{\phi(\tau^{n+1})}{X_f^n} \frac{X_f^{n+1} - X_f^n}{2\Delta y \Delta \tau} \right]$$

$$+\left(\frac{2\Delta y^2}{\varphi(\tau^{n+1})\sigma^2}\left[\beta\sum_{j=1}^{n}(X^{n-j+1}-X^{n-j})e^{-\frac{\alpha jk}{1-\alpha}}+\theta(\tau^{n+1})\left[r-\frac{\sigma^2}{2}X_f^n\right]\right.\right.$$

$$\left.\left.-\phi(\tau^{n+1})\frac{X_f^{n+1}-X_f^n}{\Delta\tau}\right]-(X^{n+1}+X^n)(1+\Delta y)+2\right)\left[\theta(\tau^{n+1})r+\varphi(\tau^{n+1})\frac{\sigma^2}{\Delta y^2}\right]$$

$$-2\beta\sum_{j=1}^{n}(v_1^{n-j+1}-v_1^{n-j})e^{-\frac{\alpha jk}{1-\alpha}}=0 \tag{53}$$

In a similar fashion, we can simplify further the above equation to obtain

$$v_2^{n+1}\left[X_f^n\left(\frac{-\theta\left(\tau^{n+1}\right)\left(r-\frac{\sigma^2}{2}\right)}{2\Delta y}-\varphi\left(\tau^{n+1}\right)\frac{\sigma^2}{2\Delta y^2}\right)+\phi\left(\tau^{n+1}\right)\frac{X_f^{n+1}-X_f^n}{2\Delta y\Delta\tau}\right]$$

$$+v_2^n\left[X_f^n\left(\frac{-\theta\left(\tau^{n+1}\right)\left(r-\frac{\sigma^2}{2}\right)}{2\Delta y}-\varphi\left(\tau^{n+1}\right)\frac{\sigma^2}{2\Delta y^2}\right)+\phi\left(\tau^{n+1}\right)\frac{X_f^{n+1}-X_f^n}{2\Delta y\Delta\tau}\right]$$

$$+\left(1-X_f^{n+1}\right)\left[X_f^n\left(\frac{\theta\left(\tau^{n+1}\right)\left(r-\frac{\sigma^2}{2}\right)}{2\Delta y}-\varphi\left(\tau^{n+1}\right)\frac{\sigma^2}{2\Delta y^2}\right)-\phi\left(\tau^{n+1}\right)\frac{X_f^{n+1}-X_f^n}{2\Delta y\Delta\tau}\right]$$

$$+\left(1-X_f^{n}\right)\left[X_f^n\left(\frac{\theta\left(\tau^{n+1}\right)\left(r-\frac{\sigma^2}{2}\right)}{2\Delta y}-\varphi\left(\tau^{n+1}\right)\frac{\sigma^2}{2\Delta y^2}\right)-\phi\left(\tau^{n+1}\right)\frac{X_f^{n+1}-X_f^n}{2\Delta y\Delta\tau}\right]$$

$$+X_f^n\left(\frac{2\Delta y^2}{\varphi(\tau^{n+1})\sigma^2}\left[\beta\sum_{j=1}^{n}(X^{n-j+1}-X^{n-j})e^{-\frac{\alpha jk}{1-\alpha}}+\theta(\tau^{n+1})\left[r-\frac{\sigma^2}{2}X_f^n\right]-\phi(\tau^{n+1})\frac{X_f^{n+1}-X_f^n}{\Delta\tau}\right]\right.$$

$$\left.-(X^{n+1}+X^n)(1+\Delta y)+2\right)\left[\theta(\tau^{n+1})r+\varphi(\tau^{n+1})\frac{\sigma^2}{\Delta y^2}\right]$$

$$-2X_f^n\beta\sum_{j=1}^{n}(v_1^{n-j+1}-v_1^{n-j})e^{-\frac{\alpha jk}{1-\alpha}}=0. \tag{54}$$

We observe that equation (54) represents a quadratic equation with complex coefficients and a constant term. At this point, the coefficients and a constant can be systematically collected for further analysis.

After factoring out the term (X_f^{n+1}) from equation (54), the resulting coefficient designated as bb can be easily obtained and estimated.

Let us begin by collecting the coefficients of X_f^{n+1} using

$$X_f^{n+1}\Bigg((v_2^{n+1}+v_2^n)\frac{\phi(\tau^{n+1})}{2\Delta y\Delta\tau}-(2-X_f^n)\frac{\phi(\tau^{n+1})}{2\Delta y\Delta\tau}$$

$$-\left[X_f^n\left(\frac{\theta(\tau^{n+1})\left(r-\dfrac{\sigma^2}{2}\right)}{2\Delta y}-\varphi(\tau^{n+1})\frac{\sigma^2}{2\Delta y^2}\right)+\frac{\phi(\tau^{n+1})X_f^n}{2\Delta y\Delta\tau}\right]$$

$$-X_f^n\left(\frac{2\Delta y^2}{\varphi(\tau^{n+1})\sigma^2}\frac{\phi(\tau^{n+1})}{\Delta\tau}+(1+\Delta y)\right)\left[\theta(\tau^{n+1})r+\varphi(\tau^{n+1})\frac{\sigma^2}{\Delta y^2}\right]\Bigg).$$

This becomes

$$bb^{n+1}=(v_2^{n+1}+v_2^n-2)\frac{\phi(\tau^{n+1})}{2\Delta y\Delta\tau}-X_f^n\left[\frac{\theta(\tau^{n+1})\left(r-\dfrac{\sigma^2}{2}\right)}{2\Delta y}-\varphi(\tau^{n+1})\frac{\sigma^2}{2\Delta y^2}\right]$$

$$-X_f^n\left(\frac{2\Delta y^2}{\varphi(\tau^{n+1})\sigma^2}\frac{\phi(\tau^{n+1})}{\Delta\tau}+(1+\Delta y)\right)\left[\theta(\tau^{n+1})r+\varphi(\tau^{n+1})\frac{\sigma^2}{\Delta y^2}\right]. \tag{55}$$

After taking the term $(X_f^{n+1})^2$ as a common factoring in equation (54), then the resulting coefficient denoted by aa, can be easily expressed in the form:

$$aa^{n+1}=\frac{\phi(\tau^{n+1})}{2\Delta y\Delta\tau}. \tag{56}$$

Finally, the constant term of the quadratic equation is aggregated, resulting in the subsequent expression denoted by cc

$$cc^{n+1}=(v_2^{n+1}+v_2^n)X_f^n\left[\frac{-\theta(\tau^{n+1})\left(r-\dfrac{\sigma^2}{2}\right)}{2\Delta y}-\varphi(\tau^{n+1})\frac{\sigma^2}{2\Delta y^2}-\frac{\phi(\tau^{n+1})}{2\Delta y\Delta\tau}\right]$$

$$+(2-X_f^n)X_f^n\left[\frac{\theta(\tau^{n+1})\left(r-\frac{\sigma^2}{2}\right)}{2\Delta y}-\varphi(\tau^{n+1})\frac{\sigma^2}{2\Delta y^2}+\frac{\phi(\tau^{n+1})}{2\Delta y\Delta\tau}\right]$$

$$+X_f^n\left(\frac{2\Delta y^2}{\varphi(\tau^{n+1})\sigma^2}\left[\beta\sum_{j=1}^{n}(X^{n-j+1}-X^{n-j})e^{-\frac{\alpha jk}{1-\alpha}}+\theta(\tau^{n+1})\right.\right.$$

$$\left.\left.\left(r-\frac{\sigma^2}{2}X_f^n\right)+\phi(\tau^{n+1})\frac{X_f^n}{\Delta\tau}\right]-X^n(1+\Delta y)+2\right)$$

$$-\left[\theta(\tau^{n+1})r+\varphi(\tau^{n+1})\frac{\sigma^2}{\Delta y^2}\right]-2X_f^n\beta\sum_{j=1}^{n}(v_1^{n-j+1}-v_1^{n-j})e^{-\frac{\alpha jk}{1-\alpha}}. \tag{57}$$

Note that equation (54) has now been simplified and its simplified version can be reformulated as:

$$aa^{n+1}(X_f^{n+1})^2+bb^{n+1}X_f^{n+1}+cc^{n+1}=0. \tag{58}$$

In order for us to resolve the issue of the quadratic equation presented above, two potential roots are obtained. However, we observed that one of the roots specifically, $\frac{-bb^{n+1}+\sqrt{(bb^{n+1})^2-4aa^{n+1}cc^{n+1}}}{2aa^{n+1}}$ falls outside the acceptable range defined by the free boundary X_f^{n+1}, since it is greater than 1. Consequently, this root is deemed nonviable, as it does not satisfy the necessary constraints, and is therefore excluded from the analysis and further consideration.

The remaining only viable root is given by $\frac{-bb^{n+1}-\sqrt{(bb^{n+1})^2-4aa^{n+1}cc^{n+1}}}{2aa^{n+1}}$. This root falls within the acceptable range and satisfies all the required conditions of the problem. Thus, it is chosen as the only valid solution in this analysis. This approach ensures that only the meaningful solutions are considered, and this is dully consistent with the free boundary conditions of X_f^{n+1}, representing the desired outcome.

4. Consistency and stability

In this section, we discuss the consistency and stability of the Crank-Nicolson method associated with the Caputo fractional derivatives for the American put options given by the relation (38). Having said that, we first deal with the consistency in the following section.

4.1 *Consistency*

To deal with the issue of consistency of the scheme considered in this manuscript, we need the following concept.

Definition 6 Let $\mathscr{F}(v_m^n, X_f^n)$ be the operator that approximates $\mathscr{L}(v, X_f)$. The local truncation error $\mathscr{T}_m^n(\bar{v}, \bar{X}_f)$ is given by the leading terms of the Taylor expansion of $\mathscr{F}(v_m^n, X_f^n)=0$, where u satisfies $\mathscr{L}(v, X_f)=0$.

We remark from the above Definition 6 that

$$\mathscr{T}_m^n(\bar{v}, \bar{X}_f) = \mathscr{F}(v_m^n, X_f^m), \quad \text{and}$$

$$\lim_{(\Delta\tau,\, \Delta y)\to(0,\, 0)} \mathscr{T}_m^n(\bar{v}, \bar{X}_f) = 0. \tag{59}$$

Let's start by choosing an arbitrary location $(y, \tau) \in [0, 4E] \times [0, T]$. Note that the mesh point (y^m, τ^n) to study the consistency of Caputo fractional PDE is given in (32) and its numerical scheme by (38). The resulting system is obtained by employing the Crank-Nicolson finite-difference method. For this purpose, we consider $\bar{v}_m^n = v(\tau^n, y_m)$ to be the exact solution for the Caputo fractional PDE and $\bar{X}_f^n = X_f^n$ to be the free boundary, respectively. Namely,

$$\mathscr{L}(v, X_f^n) = \frac{\partial^\alpha v}{\partial \tau^\alpha} - \theta(\tau)\left[rv - \left(r - \frac{\sigma^2}{2}\right)\frac{\partial v}{\partial y}\right] + \varphi(\tau)\frac{\sigma^2}{2}\frac{\partial^2 v}{\partial y^2} - \phi(\tau)\frac{X_f'(\tau)}{X_f(\tau)}\frac{\partial v}{\partial y} = 0$$

and

$$\mathscr{F}(v_n^{m+1}, X_f^{n+1}) = 2\beta\sum_{j=1}^{n}(v_m^{n-j+1} - v_m^{n-j})e^{-\frac{\alpha jk}{1-\alpha}}$$

$$= \theta\left(\tau^{n+1}\right)\left[\left(rv_m^{n+1} + rv_m^n\right) - \left(r - \frac{\sigma^2}{2}\right)\left(\frac{v_{m+1}^{n+1} - v_{m-1}^{n+1}}{2\Delta y} + \frac{v_{m+1}^n - v_{m-1}^n}{2\Delta y}\right)\right]$$

$$-\varphi\left(\tau^{n+1}\right)\frac{\sigma^2}{2}\left(\frac{v_{m-1}^{n+1} - 2v_m^{n+1} + v_{m+1}^{n+1}}{\Delta y^2} + \frac{v_{m-1}^n - 2v_m^n + v_{m+1}^n}{\Delta y^2}\right)$$

$$+\frac{\phi\left(\tau^{n+1}\right)}{X_f^n}\frac{X_f^{n+1} - X_f^n}{(\Delta\tau)}\left(\frac{v_{m+1}^{n+1} - v_{m-1}^{n+1}}{2\Delta y} + \frac{v_{m+1}^n - v_{m-1}^n}{2\Delta y}\right).$$

Having derived this result which leads us to the statement of the following consistency result.

Theorem 1 The Crank-Nicolson finite-difference scheme of the Caputo fractional derivatives defined in equations (32) is consistent with the fixed domain model (38) with order $\mathscr{O}(1) + \mathscr{O}((\Delta y)^2)$.

Proof. We implement the Taylor expansion and we rely on similar arguments to the techniques used in [1], taking into account the continuous partial derivatives of orders two and four in space and time, respectively. This helps us to show the consistency of (32).

First, we examine the consistency of fractional derivatives in equation (32). In our earlier analysis, as outlined in equation (34), we developed a scheme for the Caputo fractional derivatives corresponding to certain parts of equation (32), establishing an order of accuracy of

$$\frac{\partial^\alpha v}{\partial \tau^\alpha} = \beta\sum_{j=1}^{n}(v_m^{n-j+1} - v_m^{n-j})e^{-\frac{\alpha jk}{1-\alpha}} + \mathscr{O}(1) \text{ where } \beta = \frac{1}{k\alpha}(1 - e^{-\frac{\alpha k}{1-\alpha}}) \tag{60}$$

with the truncation denoted by

$$\mathbf{e_1} = \mathscr{O}(1). \tag{61}$$

Secondly, let us find the consistency of each of the last three right-hand side of our main equations considered in relation (32) separately, using Taylor's expansion up to order two and four in time and space, respectively.

For now, let us find the truncation error of the first term of the right-hand side of (32) by using

$$\phi\left(\tau^{n+1}\right)\sigma^2\frac{\partial^2 v}{\partial y^2} = \phi\left(\tau^{n+1}\right)\sigma^2\left(\frac{v_{m-1}^n - 2v_m^n + v_{m+1}^n}{\Delta y^2}\right)$$

$$= \frac{\phi\left(\tau^{n+1}\right)}{\Delta y^2}\sigma^2\left(v_m^n - \Delta y\frac{v_y}{1!} + (\Delta y)^2\frac{v_{yy}}{2!} - (\Delta y)^3\frac{v_{yyy}}{3!} + (\Delta y)^4\frac{v_{yyyy}}{4!} + (\Delta y)^5\right.$$

$$\left. -2v_m^n + v_m^n + \Delta y\frac{v_y}{1!} + (\Delta y)^2\frac{v_{yy}}{2!} + (\Delta y)^3\frac{v_{yyy}}{3!} + (\Delta y)^4\frac{v_{yyyy}}{4!} + (\Delta y)^5\right)$$

$$= \phi\left(\tau^{n+1}\right)\sigma^2\left(\frac{\partial^2 v}{\partial^2 y} + (\Delta y)^2\frac{1}{12}\frac{\partial^4 v}{\partial^4 y} + \mathscr{O}\left(\Delta y\right)^3\right). \tag{62}$$

Therefore the error term of (62) becomes

$$\mathbf{e_2} = \phi(\tau^{n+1})\sigma^2\left[(\Delta y)^2\frac{1}{12}\frac{\partial^4 v}{\partial^4 y} + \mathscr{O}(\Delta y)^3\right]. \tag{63}$$

Again, let us find the truncation error of the first term of the right-hand side of (32) by using

$$\theta\left(\tau^{n+1}\right)\left(\frac{\sigma^2}{2} - r\right)\frac{\partial v}{\partial y} = \theta\left(\tau^{n+1}\right)\frac{1}{2}\left(\frac{\sigma^2}{2} - r\right)\left(\frac{v_{n+1}^{m+1} - v_{n+1}^{m-1}}{2\Delta y} + \frac{v_n^{m+1} - v_n^{m-1}}{2\Delta y}\right)$$

$$= \theta\left(\tau^{n+1}\right)\frac{1}{2}\left(\frac{\sigma^2}{2} - r\right)\left(\frac{\partial v}{\partial y} + (\Delta y)^2\frac{1}{6}\frac{\partial^3 v}{\partial^3 y} + \mathscr{O}\left(\Delta y\right)^4\right). \tag{64}$$

Therefore the error term of (64) becomes

$$\mathbf{e_3} = (\Delta y)^2\frac{1}{6}\frac{\partial^3 v}{\partial^3 y} + \mathscr{O}(\Delta y)^4. \tag{65}$$

Next, let us find the truncation error of the third expression of the right-hand side of (32) by relying on the expression below:

$$\varphi\left(\tau^{n+1}\right)\frac{1}{X_f(\tau)}\frac{dX_f(\tau)}{d\tau}\frac{\partial v}{\partial y}$$

$$=\varphi\left(\tau^{n+1}\right)\frac{1}{2}\left(\frac{X_f^{n+1}(\tau)-X_f^{n}(\tau)}{\Delta\tau X_f(\tau)}\left(\frac{v_{n+1}^{m+1}-v_{n+1}^{m-1}}{2\Delta y}+\frac{v_{n}^{m+1}-v_{n}^{m-1}}{2\Delta y}\right)\right)$$

$$=\frac{\varphi\left(\tau^{n+1}\right)}{X_f(\tau)}\left(\frac{dX_f(\tau)}{d\tau}+(\Delta\tau)^2\frac{d^2X_f(\tau)}{d\tau^2}+\mathscr{O}\left((\Delta\tau)^2\right)\right)\left(\frac{\partial v}{\partial y}+(\Delta y)^2\frac{1}{6}\frac{\partial^3 v}{\partial^3 y}+\mathscr{O}(\Delta y)^4\right)$$

$$=\frac{\varphi\left(\tau^{n+1}\right)}{X_f(\tau)}\frac{dX_f(\tau)}{d\tau}\frac{\partial v}{\partial y}+\frac{\varphi\left(\tau^{n+1}\right)}{X_f(\tau)}\frac{dX_f(\tau)}{d\tau}\left((\Delta y)^2\frac{1}{6}\frac{\partial^3 v}{\partial^3 y}+\mathscr{O}(\Delta y)^4\right)$$

$$+\frac{1}{X_f(\tau)}\left((\Delta\tau)^2\frac{d^2X_f(\tau)}{d\tau^2}+\mathscr{O}\left((\Delta\tau)^2\right)\right)\left(\frac{\partial v}{\partial y}+(\Delta y)^2\frac{1}{6}\frac{\partial^3 v}{\partial^3 y}+\mathscr{O}(\Delta y)^4\right). \quad (66)$$

Therefore, the error term of (66) becomes

$$\mathbf{e_4}=\frac{\varphi(\tau^{n+1})}{X_f(\tau)}\frac{dX_f(\tau)}{d\tau}\left((\Delta y)^2\frac{1}{6}\frac{\partial^3 v}{\partial^3 y}+\mathscr{O}(\Delta y)^4\right)$$

$$+\frac{\varphi(\tau^{n+1})1}{X_f(\tau)}\left((\Delta\tau)^2\frac{d^2X_f(\tau)}{d\tau^2}+\mathscr{O}((\Delta\tau)^2)\right)\left(\frac{\partial v}{\partial y}+(\Delta y)^2\frac{1}{6}\frac{\partial^3 v}{\partial^3 y}+\mathscr{O}(\Delta y)^4\right). \quad (67)$$

Lastly, we can find the truncation error of the last term of the right-hand side of (32) using

$$rv=\frac{1}{2}(rv_{n+1}^{m}+rv_{n}^{m}). \quad (68)$$

Hence, the local truncation error of (32) can be obtained using (61) to (68). This error can be provided by the following expression:

$$\mathscr{T}_n^{m+1}(\bar{v},\bar{X}_f)=\mathbf{e_1}+\mathbf{e_2}+\mathbf{e_3}+\mathbf{e_4}=\mathscr{O}(1)+\mathscr{O}(\Delta\tau)+\mathscr{O}((\Delta y)^2). \quad (69)$$

Now, let us find the local truncation error of the boundary conditions of equations (32), (47), and (46). For us to get the boundary conditions, we use the following normal derivatives:

$$
\begin{cases}
\mathscr{L}_1(v, X_f) = v(\tau, 0) - 1 + X_f(\tau) = 0 \\[2ex]
\mathscr{L}_2(v, X_f) = \dfrac{\partial v}{\partial y}(\tau, 0) + X_f(\tau) = 0 \\[2ex]
\mathscr{L}_3(v, X_f) = -{}_0^cD_t^\alpha(1 - X_f(\tau)) + \theta(\tau^{n+1})\left[r(1 - X_f) + \left(r - \dfrac{\sigma^2}{2}\right)X_f\right] - \varphi(\tau^{n+1})\dfrac{\sigma^2}{2}\dfrac{\partial^2 v}{\partial y^2} \\[2ex]
\qquad\qquad + \dfrac{\varphi(\tau^{n+1})}{X_f(\tau)}\dfrac{dX_f(\tau)}{d\tau}\dfrac{\partial v}{\partial y} = 0
\end{cases}
\tag{70}
$$

from which we deduce the numerical boundary scheme:

$$
\begin{cases}
\mathscr{F}_1(v_{n+1}^0, X_f^{n+1}) = v_{n+1}^0 - 1 + X_f^{n+1} \\[2ex]
\mathscr{F}_2(v_{n+1}^0, X_f^{n+1}) = \dfrac{v_{n+1}^1 - v_{n+1}^{-1} + v_n^1 - v_n^{-1}}{2\Delta y} + X_f^{n+1} \\[2ex]
\mathscr{F}_3(v_{n+1}^0, X_f^{n+1}) = -\beta\sum_{j=1}^n(-X^{n-j+1} + X^{n-j})e^{-\frac{\alpha jk}{1-\alpha}} + \theta(\tau^{n+1})\left[r - \dfrac{\sigma^2}{2}X_f^{n+1}\right] \\[2ex]
\qquad\qquad -\varphi(\tau^{n+1})\dfrac{\sigma^2}{4}\left(\dfrac{v_{-1}^{n+1} - 2v_0^{n+1} + v_1^{n+1}}{\Delta y^2} + \dfrac{v_{-1}^n - 2v_0^n + v_1^n}{\Delta y^2}\right) - \dfrac{X_f^{n+1} - X_f^n}{\Delta\tau} = 0.
\end{cases}
\tag{71}
$$

By following the same steps we just used as done for relations (61) to (68) for (70) and (71), we obtain the following local truncation error

$$
\mathscr{O}(1) + \mathscr{O}(\Delta\tau) + \mathscr{O}((\Delta y)^2). \tag{72}
$$

It follows now that

$$
\mathscr{T}_1^0(\bar{v}, \bar{X}_f) = \mathscr{F}_1(V_{n+1}^0, X_f^{n+1}) = 0,
$$

$$
\mathscr{T}_2^0(\bar{v}, \bar{X}_f) = (\Delta y)^2\frac{1}{3}\frac{\partial^3 v}{\partial^3 y} + \mathscr{O}(\Delta y)^4,
$$

$$
\mathscr{T}_3^0(\bar{v}, \bar{X}_f) = \mathscr{O}(\Delta\tau) + \mathscr{O}((\Delta y)^2).
$$

As a result of (69) and (72), we can now assert that the Crank-Nicolson finite scheme provided by (38) is compatible with the fixed domain model (25) of order

$$\mathscr{O}(1)+\mathscr{O}((\Delta y)^2).$$

Thus, this proves the desired result for the consistency. □

Having dealt with the proof of the consistency associated with the corresponding problem, we can now derive the result concerning the stability of the schemes we are using in this manuscript in the following section.

4.2 *Stability*

This section presents the stability of the numerical scheme (38) under consideration. We begin by defining the stability used in the section for the sake of several concepts of stability used in the literature. In order to define the concept of stability that we deal with in this manuscript we borrow some basic notion from the papers [2, 55].

Definition 7 The numerical scheme (38) is said to be $\|v^n\|_\infty$-stable in the domain, if for every partition of the domain $[0, \infty]\times[0, T]$ we set $\Delta\tau=\dfrac{T}{N}$ and $\Delta y=\dfrac{Y}{M}$, there exists a positive constant ζ such that

$$\|v^n\|_\infty \leq \zeta, \quad \text{for } \ 0\leq n\leq N \tag{73}$$

where ζ is independent of $\Delta\tau$, Δy, and $n=1, 2, \ldots, N$.

Having defined the notion of stability that we are using here, we can state another main result of this paper in the following lemma.

Lemma 1 Let (v_n^m, X_f^n) be the computed numerical solution and for sufficiently small values of Δy, we have:

(i) X_f^n is positive and decreasing for $n=0, 1, \ldots, N$;

(ii) The vectors v_n^m have positive components for $n=0, 1, \ldots, N$;

(iii) The vectors v_n^m are decreasing w.r.t m for each fixed $n=0, 1, \ldots, N$.

Proof. The lemma can be proven following a methodology analogous to that used in Company et al. [56], Riccardo et al. [1] and Company et al. [2] and Nuugulu et al. [28]. For a detailed exposition of the proof, please refer to the corresponding discussions in these references. □

We can now state and prove another main result of general stability in the following theorem.

Theorem 2 The Crank-Nicolson finite-difference scheme for the Caputo fractional derivative as defined by equations (38) is unconditionally stable.

Proof. Since for each fixed natural integer n, we observe that the corresponding term n, v_m^n is a non-increasing sequence w.r.t m, then according to the boundary condition (38) and the positivity of X_f^n (see e.g. Lemma 2), we obtain

$$\|v^n\|_\infty = v_0^n = 1-X_f^n \leq 1, \ \text{for} \ \ 0\leq n\leq N. \tag{74}$$

Therefore, we conclude that the Crank-Nicolson scheme for the APO with Caputo fractional order derivative is unconditionally stable. Thus far, this proves the desired stability result. □

Having stated and proved both the consistency and the stability of our schemes, we are now ready to implement the numerical scheme that will be used to verify and further validate the results obtained in this manuscript.

5. Numerical result

In this section, we illustrate the previous theoretical results with numerical experiments showing the potential advantages of the proposed method, such as preserving the qualitative properties of the theoretical solution of APO such as stability and consistency. In addition, in this section, a comparison with other approaches is also presented. The APO problems (25) were solved using the following parameters:

$$r = 0.1, \ \sigma = 0.2, \ T = 1, \ \alpha = 0.5.$$

To evaluate the convergence, we calculate the error metrics, including maximum error and Root-Mean-Square Error (RMSE) in relation to the reference solution derived from our highly refined grid. The convergence rate is subsequently determined using the following formula:

i.

$$\gamma(h_1, h_2) = \frac{\ln(\mathrm{RMSE}_{h_1}) - \ln(\mathrm{RMSE}_{h_2})}{\ln(h_1) - \ln(h_2)}, \tag{75}$$

• RMSE_{h_1} and RMSE_{h_2} are the root mean square errors.

• h_1 and h_2 are the respective grids spacing.

ii.

$$\text{Convergence Rate} = \frac{\log\left(\dfrac{E_{\text{coarse}}}{E_{\text{fine}}}\right)}{\log\left(\dfrac{h_{\text{coarse}}}{h_{\text{fine}}}\right)} \tag{76}$$

where

• E_{fine}: The error associated with the finer grid, calculated using a chosen error norm, such as the maximum error or root mean square error.

• E_{coarse}: The error associated with the coarser grid, computed in the same manner as E_{fine}.

• h_{fine}: The grid spacing for the finer grid, typically represented as Δy (spatial step).

• h_{coarse}: The grid spacing for the coarser grid, similarly represented as Δy.

Having defined the convergence rate and the errors needed, we intend to now compute the errors related to the associated problem in order to validate the scheme used. For this purpose, we fix y_∞ in the table below and compute the errors for the given values for each given value N.

Table 1. Free boundary location at $t = T = 1$

$Y = y_\infty$	$N = 20$	$N = 40$	$N = 80$
1	0.72636032	0.62031929	0.50841141
2	0.72637032	0.62032529	0.50836313
4	0.72637632	0.62032829	0.50836513

We focus on determining a suitable value for the truncated boundary, $Y = y_\infty$, and subsequently analyze how the choice of $Y = y_\infty$ influences the numerical solution. A straightforward approach involves monitoring the computing values of the free boundary, X_f^n, at $t = T$. Table 1 presents a comparison of the numerical results of the sample for X_f^n obtained with varying grid step values, while keeping $\mu = 20$ and setting $y_\infty = 1$, $y_\infty = 2$, $y_\infty = 4$. The results in Table 1 reveal that, for a fixed value of $\mu = 20$, the calculated values of X_f^n remain consistent up to the first four decimal places in different values of the grid step. Based on these observations, we selected $y_\infty = 1$ for subsequent calculations. This result aligns with the preliminary numerical results derived from the implementation of explicit and implicit finite difference methods, as reported by Riccardo [49] and Riccardo et al. [1] respectively.

Having calculated the boundary solutions in the above table, we now turn our attention to compute the maximum absolute error in the table below.

Table 2. The table presents the maximum absolute errors calculated for various fractional orders of α, spanning from 0.1 to 0.9 in increments of 0.1

α	$N = 20$	$N = 40$	$N = 80$	$N = 160$
0.1	6.69e-03	2.36e-03	2.50e-03	0.00e + 00
0.2	5.34e-03	6.77e-04	6.73e-04	0.00e + 00
0.3	2.38e-03	0.00e + 00	0.00e + 00	0.00e + 00
0.4	3.07e-03	0.00e + 00	0.00e + 00	0.00e + 00
0.5	2.21e-03	0.00e + 00	0.00e + 00	0.00e + 00
0.6	1.58e-03	0.00e + 00	0.00e + 00	0.00e + 00
0.7	1.32e-03	0.00e + 00	0.00e + 00	0.00e + 00
0.8	1.68e-03	0.00e + 00	0.00e + 00	0.00e + 00
0.9	2.57e-03	0.00e + 00	0.00e + 00	0.00e + 00

Table 2 illustrates the maximum absolute errors associated with various values of fractional parameters α and different grid sizes N within a numerical method. The data reveal a consistent reduction in error as α and N increase. Specifically, the maximum absolute errors approximately halve with each doubling of N. In coarser grids $N = 10$, $N = 20$, and $N = 40$, the errors demonstrate greater variability relative to α; however, this sensitivity diminishes significantly in finer grids $N = 160$ and $N = 320$, where the errors converge to negligible levels across all values of α. This trend underscores the reliability of the method and the effectiveness of grid refinement in attaining enhanced accuracy, while also indicating a reduced sensitivity at higher resolutions.

Table 3. The table presents the convergence rates computed based on the mean values for various fractional orders of α, ranging from 0.1 to 0.9 in increments of 0.1

α	$N = 20$	$N = 40$	$N = 80$
0.1	6.90e-01	1.26e + 00	2.44e + 00
0.2	6.92e-01	1.26e + 00	2.44e + 00
0.3	6.96e-01	1.26e + 00	2.45e + 00
0.4	7.01e-01	1.27e + 00	2.45e + 00
0.5	7.08e-01	1.27e + 00	2.46e + 00
0.6	7.15e-01	1.28e + 00	2.47e + 00
0.7	7.22e-01	1.28e + 00	2.47e + 00
0.8	7.30e-01	1.29e + 00	2.48e + 00
0.9	7.53e-01	1.32e + 00	2.53e + 00

Table 4. The table presents the convergence rates calculated using the RMSE for the example problem, with fractional orders of α varying from 0.1 to 0.9 in increments of 0.1

α	$N = 20$	$N = 40$	$N = 80$
0.1	5.03e-01	9.71e-01	1.96e + 00
0.2	5.02e-01	9.70e-01	1.95e + 00
0.3	5.03e-01	9.70e-01	1.96e +00
0.4	5.05e-01	9.70e-01	1.96e + 00
0.5	5.08e-01	9.74e-01	1.96e + 00
0.6	5.13e-01	9.78e-01	1.97e + 00
0.7	5.20e-01	9.83e-01	1.97e + 00
0.8	5.31e-01	9.93e-01	1.98e + 00
0.9	5.53e-01	1.02e + 00	2.02e + 00

Table 3 illustrates the convergence rates associated with various values of α and grid sizes N in the numerical method, as determined by equation (75). For coarser grids $N = 20$, $N = 40$, and $N = 80$, the convergence rates are approximately 0.69, 1.26, and 2.44, respectively. As α increases from 0.1 to 0.9, these rates improve to 0.753, 1.32, and 2.53. This trend suggests that the method nearly achieves optimal second-order convergence as grid resolution of the grid improves. Similarly, Table 4 exhibits the convergence rates for the same grid sizes $N = 20$, $N = 40$, and $N = 80$, which begin at 0.503, 0.971, and 1.96, respectively, and further increase to 0.553, 1.02, and 2.02 with the escalation of α from 0.1 to 0.9. These results also indicate second-order convergence, consistent with the calculations derived from equation (76). The uniformity of convergence rates across varying values of α in both tables underscores the robustness of the numerical method. This characteristic ensures consistent performance regardless of the parameter α and highlights the reliability and precision of the approach, particularly as the resolution of the grid improves.

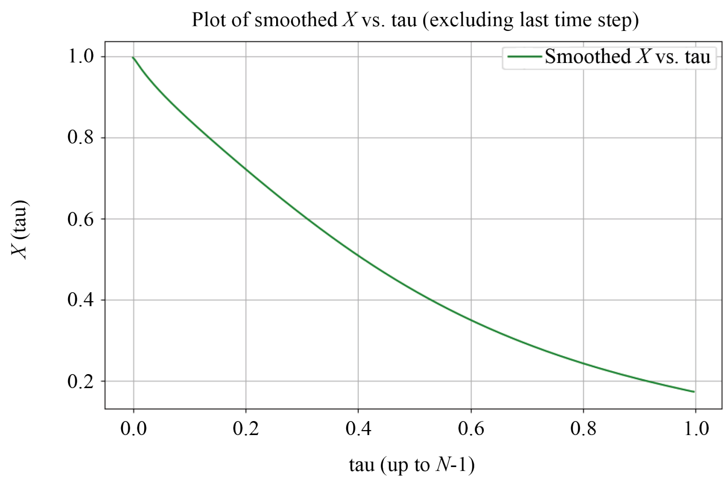

Figure 1. The figure presents the numerical results obtained using the Crank-Nicolson method, plotting X_f^n versus τ_n, with $\alpha = 0.9$

The Figures 1 and 2 present two graphs of X_f^n versus τ_n: the second graph corresponds to $\alpha = 0.5$, while the first graph also represents the same this but for $\alpha = 0.9$. These results were generated using the Crank-Nicolson finite-difference scheme with $N = 320$, $M = 80$, and $\mu = 20$. The findings suggest that the approach becomes more effective for larger values $\alpha = 0.5$. This observation aligns with the expectations, as $\alpha > 0.5$ characterizes scenarios in which the increases in the underlying stock exhibit a persistent positive correlation.

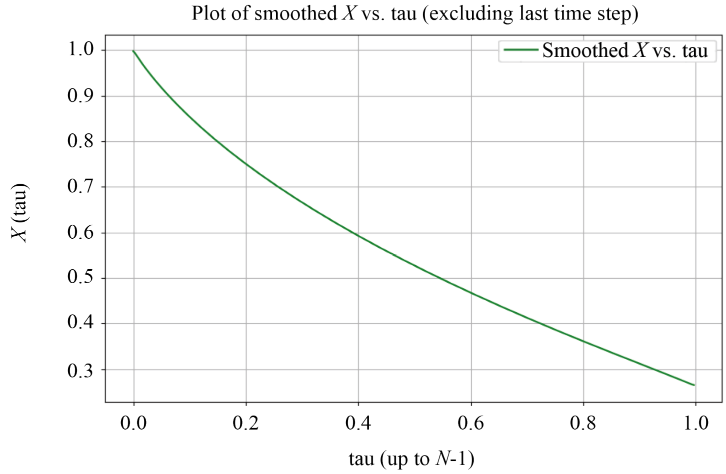

Figure 2. The figure presents the numerical results obtained using the Crank-Nicolson method, plotting X_f^n versus τ_n, with $\alpha = 0.5$

Figures 2 and 3 illustrate the results obtained from the Crank-Nicolson finite difference scheme, presenting both the graphs $2D$ and $3D$ of v_m^n versus y, respectively. The graph in Figure 4 corresponds to the case where $\alpha = 0.5$, while the graph 3 represents the same results with $\alpha = 0.9$. These results were computed with the parameters $N = 320$, $M = 80$, and $\mu = 20$. The analysis indicates that the method demonstrates improved performance for larger values of the parameter $\alpha > 0.5$. This observation is consistent with the expectations, since $\alpha > 0.5$ reflects scenarios where increases in the underlying stock exhibit a persistent positive correlation.

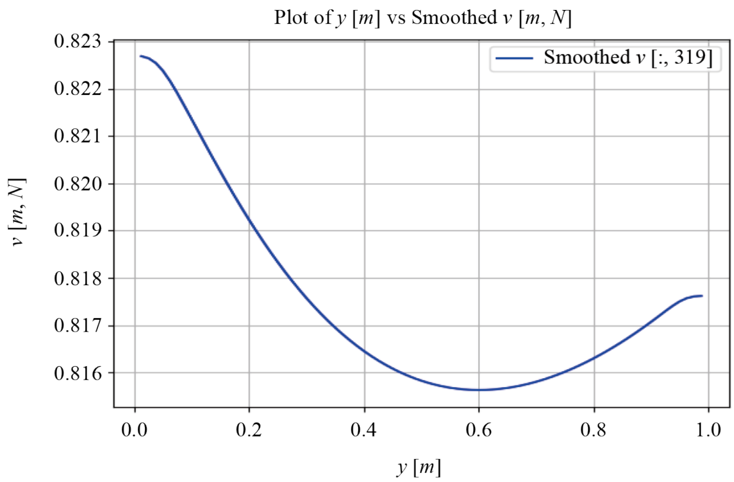

Figure 3. Maturity payoffs of an American put option, plotting v_m^n versus y, illustrating the effect of different fractional orders with $\alpha = 0.9$

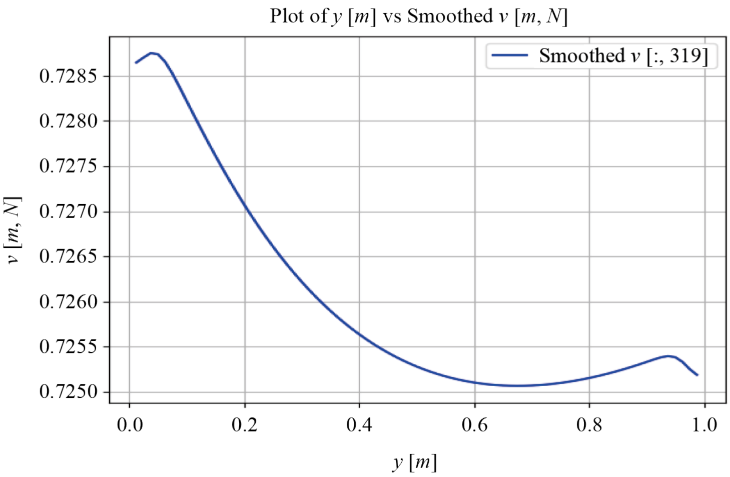

Figure 4. Maturity payoffs of an American put option, plotting v_m^n versus y, illustrating the effect of different fractional orders with $\alpha = 0.5$

We now give the profiles for the numerical solutions in the figures below.

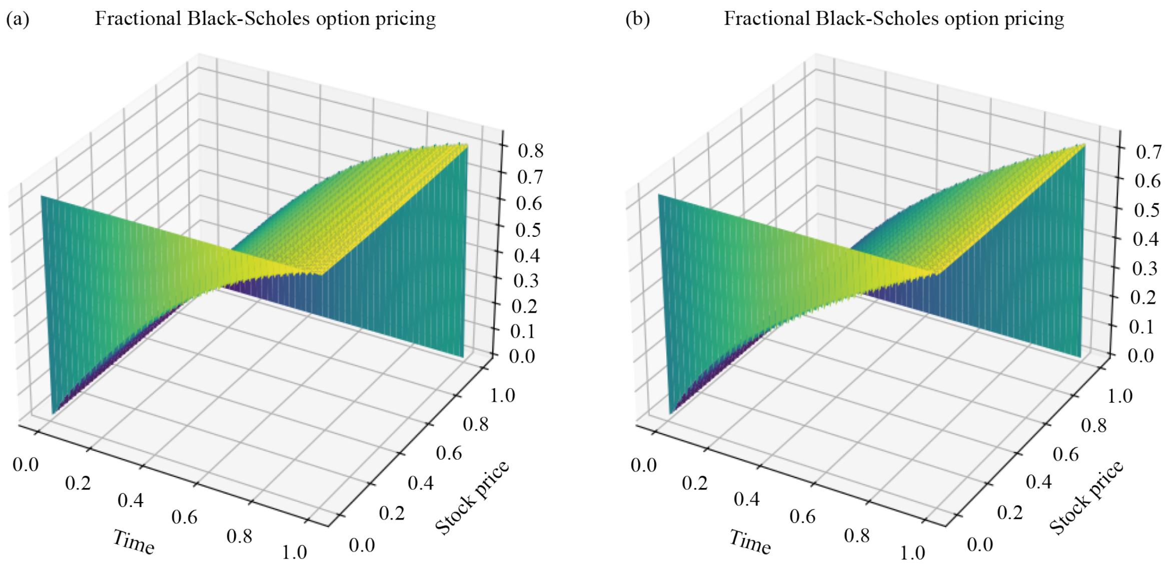

Figure 5. The figure presented shows the 3D plot of the numerical solution v_m^n, with $\alpha = 0.9$ on the left and $\alpha = 0.5$ on the right. (a) represents the 3D profiles of the numerical solution v_m^n for different fractional orders are illustrated in Figure 5a, where the plot corresponds to $\alpha = 0.9$. (b) represents the 3D profiles of the numerical solution v_m^n for different fractional orders are illustrated in Figure 5b, where the plot corresponds to $\alpha = 0.5$

The 3D profiles of the numerical solution v_m^n for different fractional orders are presented in Figure 5, where the first surface corresponds to $\alpha = 0.9$ and the second to $\alpha = 0.5$. The figure clearly illustrates the influence of the fractional parameter α on the behavior of the solution. This is to clearly demonstrate the variation in solution profiles with respect to the fractional order. As shown above, this is also to reveal how the fractional order parameter affects the amplitude and smoothness of the solution surface.

Table 5. State-of-the-art research gap analysis for fractional Black-Scholes models in American option pricing

Author	Research focus and methodology	Key findings and strengths	Limitations	Identified research gap
Company et al. [56]	Front-fixing method for classical American options; numerical analysis of front-fixing Finite-Difference (FD) schemes	Validated convergence and stability for classical free-boundary PDEs; rigorous error analysis; computationally efficient	Limited to non-fractional, non-jump models	No extension to fractional/jump-diffusion frameworks
Fazio et al. [49]	Richardson's extrapolation and error estimator for American puts; front-fixing finite difference scheme with Richardson extrapolation	Improved accuracy via a posteriori error estimation; validated convergence rates; explicit error control; efficient for classical Black-Scholes (BS) models	Limited to integer-order PDEs; no fractional extensions	Lack of error estimators for fractional free-boundary problems
Fazio et al. [1]	Implicit finite difference method for American puts; front-fixing implicit FD scheme; nonlinear solver (Newton-Raphson)	Stable convergence for free boundaries under classical BS model; robust for non-smooth payoffs; handles early exercise constraints	Computationally intensive for fine grids; no stochastic volatility	No extension to fractional operators or multi-asset models
Company et al. [15]	American options under jump-diffusion models; front-fixing Exponential Time Difference (ETD) method	Stabilized scheme for jump-induced discontinuities; handles jumps; robust for non-smooth payoffs	High runtime for fine grids; no fractional operators	Integration of jumps with fractional calculus unexplored
Kumar et al. [21]	Numerical computation of fractional BS equation; finite difference method for fractional PDEs	Solved fractional BS for European options; early work on fractional BS; validated accuracy	Focused on European options; no free boundaries	No treatment of American options or early exercise
Nuugulu et al. [28]	Robust numerical scheme for American options under time-fractional Black-Scholes model; front-fixing method with finite differences; simultaneous boundary/price solve; consistent, stable, convergent scheme for free boundaries in fractional PDEs	Handles non-locality of fractional derivatives; guarantees positivity	First-order in time; limited to time-fractional models	Higher-order schemes, space-time fractional models
Ali et al. [40]	A front fixing Crank-Nicolson finite-deference for the American put options model; front-fixing method with finite differences; simultaneous boundary/price solve; consistent, stable, convergent scheme for free boundaries in Caputo fractional PDEs	Handles non-locality of Caputo Fabrizio fractional derivatives; guarantees positivity	First order in time; limited to time-fractional models	Addressed gaps: Simultaneous free boundary computation under fractional calculus. Remaining gaps: Higher-order schemes, space-time fractional models; future research should integrate machine learning with stochastic volatility models for precise, data-driven parameter estimation, enhancing accuracy and realism

A comparative summary of recent contributions in the field of fractional Black-Scholes models for American option pricing is presented in Table 5. The table highlights the current state-of-the-art approaches, their methodologies, and the specific research gaps that persist in this domain. Notably, while several studies have introduced fractional-order formulations to capture memory effects and market irregularities, most of them focus primarily on European options and overlook the numerical stability and convergence characteristics crucial for American options. The proposed method in this work addresses these gaps by providing a more robust numerical framework that ensures both convergence and stability across varying fractional orders. This improvement reinforces the reliability of the fractional Black-Scholes model for practical financial applications.

6. Managerial and policy implications

This research introduces a transformation framework designed for financial professionals and policymakers that addresses critical challenges in the pricing of American options and risk management.

For portfolio managers, the integration of fractional calculus allows for precise valuation by concurrently calculating optimal exercise boundaries and option premiums. This methodology effectively captures long-range dependencies and non-local effects in asset price dynamics, thereby enhancing hedging strategies for volatile assets and complex derivatives [57–60]. Furthermore, the front-fixing algorithm improves efficiency by minimizing computational overhead while ensuring numerical stability [61–64]. Financial institutions can leverage this framework for real-time dynamic hedging of large portfolios, even among turbulent markets [65–73], and for cost-effective evaluations of path-dependent options, such as convertible bonds, without the need for computationally intensive simulations.

From a regulatory point of view, the framework aligns with empirical market behavior by incorporating memory effects and anomalous diffusion. This provides policymakers with valuable tools to mitigate systemic risks in derivatives markets as indicated in [74–79]. The consistency and stability support the standardized fair value measurements under regulatory frameworks, particularly for illiquid or long-dated options, where traditional models often underestimate tail risks. In addition, the robustness improves stress testing protocols for evaluating institutional resilience [80–82]. Regulatory pilots can also support the development of innovative financial instruments, such as climate-linked derivatives, within fractal-structured markets such as cryptocurrencies, fostering financial innovation while maintaining regulatory oversight through rigorous validation.

Despite these advancements, persisting challenges require resolution, notably the computational complexity inherent to non-local fractional operators and the sensitivity in parameter calibration, particularly for the parameter α which is known as the fractional order.

Future research could investigate the integration of machine learning techniques for data-driven parameter estimation or combine this framework with stochastic volatility models to improve realism. By bridging fractional calculus with practical finance, this study lays the groundwork for more transparent, efficient, and resilient financial markets that will benefit industry practitioners and regulatory bodies alike.

6.1 *Limitations of the study*

The proposed numerical scheme offers significant advances in the pricing of American options within the fractional Black-Scholes framework; however, several limitations merit careful consideration.

A primary challenge arises from the computational complexity associated with the non-local characteristics of fractional derivatives. Although the front-fixing method reduces the necessity of iterative boundary adjustments, the scheme's reliance on dense matrix operations for time-fractional discretization may adversely affect stability, particularly in high-dimensional or multi-asset contexts.

Moreover, the accuracy is highly sensitive to the precise calibration of the fractional order, which dictates the memory effects of the underlying process. Estimating this order from market data presents challenges due to inherent noise and dynamics, potentially undermining the reliability of the results.

Furthermore, the model presumes constant parameters such as interest rates, volatility, and dividend yields even if actual markets frequently exhibit stochastic or regime-switching behaviors that remain unaccounted for within this framework. The theoretical analysis also assumes certain smoothness and differentiability conditions, including the differentiability of the function up to the fractional order α. However, these assumptions may not hold in markets characterized by abrupt shocks or discontinuous price trajectories by limiting the method's applicability during periods of market turbulence. Although the numerical experiments were carried out in line with theoretical expectations, they were performed under controlled parameters, necessitating further validation against real-market data, especially for long-dated options or assets exhibiting heavy-tailed returns, to assess practical effectiveness.

This study predominantly employs Caputo-Fabrizio's fractional derivative; however, conducting a comparative analysis using alternative fractional definitions, such as Caputo or Riemann-Louville, could yield a more comprehensive theoretical foundation, as different frameworks of fractional calculus may influence pricing accuracy, see for instance [83] where a comparative study has been discussed. Lastly, although the method is specifically designed for American put options, extending it to encompass other option types, such as American calls or hybrid derivatives with early exercise and path-dependent features, would require additional algorithmic refinements.

7. Conclusion & discussion

Over the last decade, the field of financial modeling has made substantial advances, particularly the introduction of various mathematical frameworks that aim to capture the complex dynamics of financial markets. Among these, fractional calculus-based models have emerged as equally powerful tool, balancing the need to explain the intricate behaviors and evolutions of stock market while maintaining mathematical tractability. Despite the significant mathematical challenges associated with designing analytic solutions for fractional models, our work addresses this gap by proposing a robust numerical scheme to solve time-fractional Black-Scholes equations to price American put option contracts.

This study introduces a numerical approach by heavily relying in the front-fixing algorithm, which simplifies the inherent complexity of early exercise boundaries by transforming them into fixed boundaries. This transformation enables simultaneous computation of optimal exercise boundaries and the fair premiums charged for the options. We emphasize that the consistency, stability, and convergence up to order $\mathbf{O}(1, \Delta y^2)$ and the theoretical properties of the proposed scheme have been rigorously demonstrated. Moreover, the scheme guarantees the positivity and monotonicity of the option premium solutions v_n^m and the free boundary X_f^n under all potential market conditions.

To validate the theoretical assertions, a numerical experiment was conducted, simulating a practical scenario of the American put option with market particular parameters: $r = 0.10$, $T = 1$, and $\sigma = 0.20$. Importantly, our results align with findings reported in the existing literature, underscoring the reliability and effectiveness of fractional calculus frameworks for modeling financial markets. From a broader perspective, this work supports the consensus that fractional calculus provides a comprehensive framework for capturing and explaining stylized facts of market dynamics, which often elude classical modeling approaches. A particularly notable finding is that the proposed model delivers more accurate results when the fractional order $\alpha > 0.5$. This is dully consistent with the view that markets exhibit long memory. Under such conditions, the underlying fractal processes display persistence and positive correlation. Although the proposed method demonstrates robustness, efficiency, and accuracy in pricing American options, it also opens avenues for future research. Upcoming efforts will focus on calibrating similar fractional models to real-time market data and developing higher-order numerical schemes to price American put options and other related financial instruments. By addressing these challenges, we aim to further enhance the practical applicability and precision of fractional-calculus-based financial models, contributing to the broader field of quantitative finance.

Conflict of interest

The authors declare no competing financial interest.

References

[1] Fazio R, Insana A, Jannelli A. A front-fixing implicit finite difference method for the American put options model. *Mathematical and Computational Applications*. 2021; 26(2): 30. Available from: https://doi.org/10.3390/mca26020030.

[2] Egorova VN, Jódar L. Solving American option pricing models by the front fixing method: numerical analysis and computing. *Abstract and Applied Analysis*. 2014; 2014: 146745. Available from: https://doi.org/10.1155/2014/146745.

[3] Black F, Scholes M. The pricing of options and corporate liabilities. *Journal of Political Economy*. 1973; 81(3): 637-654. Available from: https://doi.org/10.1086/260062.

[4] Merton RC. Theory of rational option pricing. *The Bell Journal of Economics and Management Science*. 1973; 4(1): 141-183.

[5] Schwartz ES. The valuation of warrants: implementing a new approach. *Journal of Financial Economics*. 1977; 4(1): 79-93. Available from: https://doi.org/10.1016/0304-405X(77)90037-X.

[6] Brennan MJ, Schwartz ES. The valuation of American put options. *The Journal of Finance*. 1977; 32(2): 449-462. Available from: https://doi.org/10.2307/2326779.

[7] Brennan MJ, Schwartz ES. Finite difference methods and jump processes arising in the pricing of contingent claims: a synthesis. *Journal of Financial and Quantitative Analysis*. 1978; 13(3): 461-474. Available from: https://doi.org/10.2307/2330152.

[8] Jaillet P, Lamberton D, Lapeyre B. Variational inequalities and the pricing of American options. *Acta Applicandae Mathematicae*. 1990; 21(3): 263-289. Available from: https://doi.org/10.1007/BF00047211.

[9] Han H, Wu X. A fast numerical method for the Black-Scholes equation of American options. *SIAM Journal on Numerical Analysis*. 2003; 41(6): 2081-2095. Available from: https://doi.org/10.1137/S0036142901390238.

[10] Pantazopoulos KN, Houstis EN, Kortesis S. Front-tracking finite difference methods for the valuation of American options. *Computational Economics*. 1998; 12(3): 255-273. Available from: https://doi.org/10.1023/A:1008695215988.

[11] Tangman DY, Gopaul A, Bhuruth M. A fast high-order finite difference algorithm for pricing American options. *Journal of Computational and Applied Mathematics*. 2008; 222(1): 17-29. Available from: https://doi.org/10.1016/j.cam.2007.10.044.

[12] Al Kathiri S, Abdullah FA, Abd Hamid NN, Bashier E, Bhat AA, Sunny DA. Applications of the nonstandard finite difference method to a fractional model explaining diabetes mellitus and its complications. *Contemporary Mathematics*. 2024; 5(4): 6296-6319. Available from: https://doi.org/10.37256/cm.5420245701.

[13] Abouelregal AE, Alhassan Y, Alsaeed SS, Marin M, Elzayady ME. MGT photothermal model incorporating a generalized Caputo fractional derivative with a tempering parameter: application to an unbounded semiconductor medium. *Contemporary Mathematics*. 2024; 5(4): 6556-6581. Available from: https://doi.org/10.37256/cm.5420245963.

[14] Alkhezi Y, Awad Y, Amin K, Mghames R. On the solutions of nonlinear implicit ω-Caputo fractional order ordinary differential equations with two-point fractional derivatives and integral boundary conditions in Banach algebra. *Contemporary Mathematics*. 2024; 5(4): 4805-4835. Available from: https://doi.org/10.37256/cm.5420245216.

[15] Company R, Egorova VN, Jódar L. A front-fixing ETD numerical method for solving jump-diffusion American option pricing problems. *Mathematics and Computers in Simulation*. 2021; 189: 69-84. Available from: https://doi.org/10.1016/j.matcom.2020.07.015.

[16] Crank J. *Free and Moving Boundary Problems*. Oxford University Press; 1984.

[17] Holmes AD, Yang H, Zhang S. A front-fixing finite element method for the valuation of American options with regime switching. *International Journal of Computer Mathematics*. 2012; 89(9): 1094-1111. Available from: https://doi.org/10.1080/00207160.2012.663911.

[18] Wu L, Kwok Y-K. A front-fixing finite difference method for the valuation of American options. *Journal of Financial Engineering*. 1997; 6(4): 83-97.

[19] Zhu Y-L, Chen B-M, Ren H, Xu H. Application of the singularity-separating method to American exotic option pricing. *Advances in Computational Mathematics*. 2003; 19(1): 147-158. Available from: https://doi.org/10.1023/A:1022835722199.

[20] Landau HG. Heat conduction in a melting solid. *Quarterly of Applied Mathematics*. 1950; 8(1): 81-94. Available from: https://doi.org/10.1090/qam/33441.

[21] Kumar S, Kumar D, Singh J. Numerical computation of fractional Black-Scholes equation arising in financial market. *Egyptian Journal of Basic and Applied Sciences*. 2014; 1(3-4): 177-183. Available from: https://doi.org/10.1016/j.ejbas.2014.10.003.

[22] Nuugulu SM, Gideon F, Patidar KC. A robust numerical scheme for a time-fractional Black-Scholes partial differential equation describing stock exchange dynamics. *Chaos, Solitons & Fractals*. 2021; 145: 110753. Available from: https://doi.org/10.1016/j.chaos.2021.110753.

[23] Yavuz M, Özdemir N. A different approach to the European option pricing model with new fractional operator. *Mathematical Modelling of Natural Phenomena*. 2018; 13(1): 12. Available from: https://doi.org/10.1051/mmnp/2018009.

[24] Atangana A, Baleanu D. New fractional derivatives with nonlocal and non-singular kernel: theory and application to heat transfer model. *arXiv:1602.03408*. 2016. Available from: https://doi.org/10.48550/arXiv.1602.03408.

[25] Baleanu D, Güvenç ZB, Machado JAT. *New Trends in Nanotechnology and Fractional Calculus Applications*. Springer; 2010.

[26] Caputo M, Fabrizio M. A new definition of fractional derivative without singular kernel. *Progress in Fractional Differentiation and Applications*. 2015; 1(2): 73-85.

[27] Qureshi S, Rangaig NA, Baleanu D. New numerical aspects of Caputo-Fabrizio fractional derivative operator. *Mathematics*. 2019; 7(4): 374. Available from: https://doi.org/10.3390/math7040374.

[28] Nuugulu SM, Gideon F, Patidar KC. A robust numerical simulation of a fractional Black-Scholes equation for pricing American options. *Journal of Nonlinear Mathematical Physics*. 2024; 31(1): 40. Available from: https://doi.org/10.1007/s44198-024-00207-y.

[29] Ali Z, Abebe MA, Nazir T. A front fixing implicit finite difference for the American put options model. *arXiv:2512.06214*. 2022. Available from: https://doi.org/10.48550/arXiv.2512.06214.

[30] Anderson DR, Ulness DJ. Newly defined conformable derivatives. *Advances in Dynamical Systems and Applications*. 2015; 10(2): 109-137.

[31] Khalil R, Al Horani M, Yousef A, Sababheh M. A new definition of fractional derivative. *Journal of Computational and Applied Mathematics*. 2014; 264: 65-70. Available from: https://doi.org/10.1016/j.cam.2014.01.002.

[32] Abu-Shady M, Kaabar MKA. A novel computational tool for the fractional-order special functions arising from modeling scientific phenomena via Abu-Shady-Kaabar fractional derivative. *Computational and Mathematical Methods in Medicine*. 2022; 2022: 2138775. Available from: https://doi.org/10.1155/2022/2138775.

[33] Yang X-J. *General Fractional Derivatives: Theory, Methods and Applications*. Chapman and Hall/CRC; 2019.

[34] Li C, Qian D, Chen YQ. On Riemann-Liouville and Caputo derivatives. *Discrete Dynamics in Nature and Society*. 2011; 2011: 562494. Available from: https://doi.org/10.1155/2011/562494.

[35] Atangana A, Secer A. A note on fractional order derivatives and table of fractional derivatives of some special functions. *Abstract and Applied Analysis*. 2013; 2013: 279681. Available from: https://doi.org/10.1155/2013/279681.

[36] Jumarie G. Modified Riemann-Liouville derivative and fractional Taylor series of nondifferentiable functions further results. *Computers & Mathematics with Applications*. 2006; 51(9-10): 1367-1376. Available from: https://doi.org/10.1016/j.camwa.2006.02.001.

[37] Jumarie G. Stock exchange fractional dynamics defined as fractional exponential growth driven by (usual) Gaussian white noise. Application to fractional Black-Scholes equations. *Insurance: Mathematics and Economics*. 2008; 42(1): 271-287. Available from: https://doi.org/10.1016/j.insmatheco.2007.03.001.

[38] Jumarie G. Derivation and solutions of some fractional Black-Scholes equations in coarse-grained space and time. Application to Merton's optimal portfolio. *Computers & Mathematics with Applications*. 2010; 59(3): 1142-1164. Available from: https://doi.org/10.1016/j.camwa.2009.05.015.

[39] Jumarie G. Merton's model of optimal portfolio in a Black-Scholes market driven by a fractional Brownian motion with short-range dependence. *Insurance: Mathematics and Economics*. 2005; 37(3): 585-598. Available from: https://doi.org/10.1016/j.insmatheco.2005.06.003.

[40] Ali Z, Abebe MA, Nazir T. Strong convergence of Euler-type methods for nonlinear fractional stochastic differential equations without singular kernel. *Mathematics*. 2024; 12(18): 2890. Available from: https://doi.org/10.3390/math12182890.

[41] Baleanu D, Mousalou A, Rezapour S. A new method for investigating approximate solutions of some fractional integro-differential equations involving the Caputo-Fabrizio derivative. *Advances in Difference Equations*. 2017; 2017(1): 51. Available from: https://doi.org/10.1186/s13662-017-1088-3.

[42] Losada J, Nieto JJ. Properties of a new fractional derivative without singular kernel. *Progress in Fractional Differentiation and Applications*. 2015; 1(2): 87-92.

[43] Øksendal B. *Stochastic Differential Equations: An Introduction with Applications*. 6th ed. Springer; 2003.
[44] Bastianello L, Chateauneuf A, Cornet B. Put-call parities, absence of arbitrage opportunities, and nonlinear pricing rules. *Mathematical Finance*. 2024; 34(4): 1242-1262. Available from: https://doi.org/10.1111/mafi.12433.
[45] Cox AMG, Hoeggerl C. Model-independent no-arbitrage conditions on American put options. *Mathematical Finance*. 2016; 26(2): 431-458. Available from: https://doi.org/10.1111/mafi.12058.
[46] Kwok YK. *Mathematical Models of Financial Derivatives*. Springer; 2008.
[47] Kim E, Nie T, Rutkowski M. Arbitrage-free pricing of American options in nonlinear markets. *arXiv:1804.10753*. 2018. Available from: https://doi.org/10.48550/arXiv.1804.10753.
[48] Bollinger TR, Melick WR, Thomas CP. Principled pasting: attaching tails to risk-neutral probability density functions recovered from option prices. *Quantitative Finance*. 2023; 23(12): 1751-1768. Available from: https://doi.org/10.1080/14697688.2023.2272677.
[49] Fazio R. American put option: Richardson's extrapolation and a posteriori error estimator for a front-fixing finite difference scheme. *Applied Mathematics E-Notes*. 2020; 20: 445-457.
[50] Nielsen BF, Skavhaug O, Tveito A. Penalty and front-fixing methods for the numerical solution of American option problems. *Journal of Computational Finance*. 2002; 5(4): 69-98. Available from: https://doi.org/10.21314/JCF.2002.084.
[51] Ševčovič D. An iterative algorithm for evaluating approximations to the optimal exercise boundary for a nonlinear Black-Scholes equation. *Canadian Applied Mathematics Quarterly*. 2007; 15(1): 77-97.
[52] Zhang J, Zhu S. A hybrid finite difference method for valuing American puts. In: *Proceedings of the World Congress on Engineering*. London, U.K.: WCE; 2009. p.1131-1136.
[53] Kangro R, Nicolaides R. Far field boundary conditions for Black-Scholes equations. *SIAM Journal on Numerical Analysis*. 2000; 38(4): 1357-1368. Available from: https://doi.org/10.1137/S0036142999355921.
[54] Wilmott P, Dewynne J, Howison S. *Option Pricing: Mathematical Models and Computation*. Oxford Financial Press; 1993.
[55] Company R, Jódar L, Pintos J-R. A consistent stable numerical scheme for a nonlinear option pricing model in illiquid markets. *Mathematics and Computers in Simulation*. 2012; 82(10): 1972-1985. Available from: https://doi.org/10.1016/j.matcom.2010.04.026.
[56] Company R, Egorova VN, Jódar L. Solving American option pricing models by the front fixing method: numerical analysis and computing. *Abstract and Applied Analysis*. 2014; 2014: 146745. Available from: https://doi.org/10.1155/2014/146745.
[57] Ogundu PG. The strategic implications of financial derivatives in hedging corporate exposure to global economic volatility. *World Journal of Advanced Research and Reviews*. 2025; 25(2): 1218-1234. Available from: https://doi.org/10.30574/wjarr.2025.25.2.0482.
[58] Purnomo H, Sugeng B, Handayati P. Strategy of derivatives hedging: maintaining and increasing firm value amidst market volatility in indonesia. *Shafin: Sharia Finance and Accounting Journal*. 2024; 4(2): 66-84. Available from: https://doi.org/10.19105/sfj.v4i2.15502.
[59] Windcliff H, Forsyth PA, Vetzal KR. Pricing methods and hedging strategies for volatility derivatives. *Journal of Banking & Finance*. 2006; 30(2): 409-431. Available from: https://doi.org/10.1016/j.jbankfin.2005.04.025.
[60] Jakhongir D, Raju NSVN. The effectiveness of hedging strategies in volatile markets: literature review. In: *Recent Trends in Commerce and Business Management*. Research Floor; 2025.
[61] Zhang K, Song H, Li J. Front-fixing FEMs for the pricing of American options based on a PML technique. *Applicable Analysis*. 2015; 94(5): 903-931. Available from: https://doi.org/10.1080/00036811.2014.907563.
[62] Egorova VN, Tan S-H, Lai C-H, Company R, Jódar L. Moving boundary transformation for American call options with transaction cost: finite difference methods and computing. *International Journal of Computer Mathematics*. 2017; 94(2): 345-362. Available from: https://doi.org/10.1080/00207160.2015.1108409.
[63] Soleymani F. Numerical analysis of novel finite difference methods. In: *Novel Methods in Computational Finance*. Springer; 2017. p.171.
[64] Company R, Egorova VN, Jódar L. An ETD method for vulnerable American options. *Mathematics*. 2024; 12(4): 602. Available from: https://doi.org/10.3390/math12040602.
[65] Odunaike A. Integrating real-time financial data streams to enhance dynamic risk modeling and portfolio decision accuracy. *International Journal of Computer Applications in Technology and Research*. 2025; 14(8): 1-16. Available from: https://doi.org/10.7753/IJCATR1408.1001.

[66] Asif SSM. Create an AI-based model for dynamic risk management in equity portfolios that accounts for extreme market events (eg, pandemics, financial crises). *Journal of Information Systems Engineering and Management*. 2025; 10(20s). Available from: https://doi.org/10.52783/jisem.v10i20s.3010.

[67] Kumar K. Cross-asset correlation shifts in crisis periods: a framework for portfolio hedging. *Journal of Data Analysis and Critical Management*. 2025; 1(1): 40-51. Available from: https://doi.org/10.64235/abgwyh50.

[68] Khatwani R, Shah P, Sekhar R, Penubadi HR, Mitra PK, Shrotriya L, et al. Deep learning models for hedging strategies in derivative markets. In: *2024 International Conference on Intelligent Systems and Advanced Applications (ICISAA)*. Pune, India: IEEE; 2024. p.1-7.

[69] Peters A. Risk-sensitive fractional HJB framework for tokenized asset markets in the digital economy. *SSRN*. 2025. Available from: https://dx.doi.org/10.2139/ssrn.5532244.

[70] Devan M, Thirunavukkarasu K, Shanmugam L. Algorithmic trading strategies: real-time data analytics with machine learning. *Journal of Knowledge Learning and Science Technology*. 2023; 2(3): 522-546. Available from: https://doi.org/10.60087/jklst.vol2.n3.p546.

[71] Jiang G, Hong LJ, Shen H. Real-time derivative pricing and hedging with consistent metamodels. *INFORMS Journal on Computing*. 2024; 36(5): 1168-1189. Available from: https://doi.org/10.1287/ijoc.2023.0292.

[72] Popovska E, Georgieva-Tsaneva G. Fractal-based robotic trading strategies using detrended fluctuation analysis and fractional derivatives: a case study in the energy market. *Fractal and Fractional*. 2024; 9(1): 5. Available from: https://doi.org/10.3390/fractalfract9010005.

[73] Yang J, Tang Y, Li Y, Zhang L, Zhang H. Dynamic hedging strategies in derivatives markets with LLM-driven sentiment and news analytics. *arXiv:2504.04295*. 2025. Available from: https://doi.org/10.48550/arXiv.2504.04295.

[74] Scholes MS. Global financial markets, derivative securities, and systemic risks. *Journal of Risk and Uncertainty*. 1996; 12(2): 271-286. Available from: https://doi.org/10.1007/BF00055798.

[75] Adeloye FC, Olawoyin OM. Advanced financial derivatives in managing systemic risk and liquidity shocks in interconnected global markets. *International Journal of Science and Research Archive*. 2025; 15(2): 1017-1037. Available from: https://doi.org/10.30574/IJSRA.2025.15.2.1500.

[76] Wellink N. Mitigating systemic risk in OTC derivative markets. *Financial Stability Review*. 2010; 14: 131-135.

[77] Schwarcz SL. Derivatives and collateral: balancing remedies and systemic risk. *University of Illinois Law Review*. 2015; 2015: 699-720.

[78] Fulga ECN. Exploring the dynamics of derivative markets. a comprehensive study on futures, options, and swaps in modern finance. *Young Economists Magazine*. 2024; 43: 97-108.

[79] Markose SM. *Systemic Risk From Global Financial Derivatives: A Network Analysis of Contagion and Its Mitigation With Super-Spreader Tax*. International Monetary Fund; 2012.

[80] Marmo R, Adey BT, Celentano G. Stress testing hospitals using service measures and resilience indicators. *International Journal of Disaster Risk Reduction*. 2025; 123(9): 105492. Available from: https://doi.org/10.1016/j.ijdrr.2025.105492.

[81] Galbusera L, Ward D, Giannopoulos G. *Developing Stress Tests to Improve the Resilience of Critical Infrastructures: A Feasibility Analysis*. Publications Office of the European Union; 2015.

[82] Osterrieder J, Arakelian V, Coita IF, Hadji-Misheva B, Kabasinskas A, Machado M, et al. An overview-stress test designs for the evaluation of AI and ML models under shifting financial conditions to improve the robustness of models. *SSRN Electronic Journal*. 2023. Available from: https://doi.org/10.2139/ssrn.4634266.

[83] Khurshaid A, Khurshaid H. Comparative analysis and definitions of fractional derivatives. *Journal of Biological and Environmental Sciences*. 2023; 17(2): 2276-2285. Available from: https://doi.org/10.5281/zenodo.10000000.